



## ROBOMINERS DELIVERABLE D3.3

### ROBOMINER SUBSYSTEMS AND COMPONENTS LABORATORY TEST REPORT

*Summary:*

This document presents Robominer\_(RM1) final design and provides a changelog on the requirement specification. It also provides information on the full scale subsystems laboratory tests performed in the development and design phase of RM1.

*Authors:*

Jussi Aaltonen, TAU

Eetu Friman, TAU

Kalle Hakonen, TAU

Tuomas Salomaa, TAU

Hannes Räme, TAU





Anton Laine, TAU


This project has received funding from the European Union's Horizon 2020 research and innovation programme under grant agreement n° 820971.



<b>Title:</b>	Robominer subsystems and components laboratory test report		
<b>Lead beneficiary:</b>	TAU		
<b>Other beneficiaries:</b>	UPM, TALL, MUL, RCI, RBINS, LRC, UNIM, GeoZS		
<b>Due date:</b>	M36		
<b>Nature:</b>	Public		
<b>Diffusion:</b>	all Partners		
<b>Status:</b>	Working Document		
<b>Document code:</b>			
<b>Revision history</b>	<i>Author</i>	<i>Delivery date</i>	<i>Summary of changes and comments</i>
<b>Version 01</b>	TAU	03.06.2022	Base document
<b>Version 02</b>	TAU	17.06.2022	Revision after internal review
<b>Version 03</b>			
<b>Final version</b>			

Modifications between versions	
Version 1	The base document
Version 2	Corrections, additions, restructuring
Version 3	

Approval status				
	Name	Function	Date	Signature
<b>Deliverable responsible</b>	Jussi Aaltonen		17.06.2022	
<b>WP leader</b>	Jussi Aaltonen		17.06.2022	
<b>Reviewer</b>	Miguel Hernando		16.06.2022	
<b>Reviewer</b>	Asko Ristolainen		7.06.2022	

<b>Project Coordinator</b>	Claudio Rossi		17.06.2022	
----------------------------	---------------	--	------------	---

This document reflects only the author's view and the European Commission is not responsible for any use that may be made of the information it contains.

DiffusionList		
Partner_name	Name	e-mail
All partners	-	robominers_all@autolistas.upm.es

## EXECUTIVE SUMMARY

In ROBOMINERS project workpackage 3 designs and develops the hardware subsystems and structural components for the Robominer. This document reports laboratory tests made during the development process of the subsystems.

Tests were conducted to several critical system components related to the water hydraulic powertrain of the robot, its electronics and its communication systems. Tests concentrate in studying the dynamics of hydraulic valves and hydraulic servoactuators, studying the pressure tolerance of electronics which was required to develop pressure tolerant electronic systems for RM1 and testing the reliability of the robot communications network. All components and subsystems will be further tested in real application when RM1 is completed and tested both in laboratory and relevant operational environment.

Tests conducted proved design solution feasible and development goals to be reached.



## TABLE OF CONTENTS

Table of contents.....	5
List of figures .....	6
List of tables .....	9
1. Introduction.....	10
2. Robominer prototype RM1 .....	11
2.1. Design changes to RM1 during the development in WP3.....	11
2.2. RM1 structure and dimensions.....	11
2.3. RM1 Subsystems .....	14
2.3.1. Hydraulic system .....	15
2.3.2. Low level control and communications systems .....	20
2.3.3. Power system .....	23
2.3.4. Auxiliary systems .....	24
3. Component and subsystems laboratory tests .....	25
3.1. Water Hydraulics Components .....	25
3.1.1. Water Hydraulic 4/3-Valves .....	25
3.1.2. Water Hydraulic 2/2-Valves .....	26
3.1.3. Proportional 4-way valve composed of on/off valves .....	33
3.1.4. Screw Propulsion Units.....	36
3.1.5. Hydraulic muscles.....	41
3.2. Electronic Systems.....	43
3.2.1. Pressure Tolerance of Electronic Components.....	43
3.2.2. Valve controller board.....	46
3.2.3. Electronic pressure regulator.....	47
3.2.4. Pressure Tolerant Sensors.....	49
3.2.5. Communication Network .....	51
4. Effector and multicoupling Laboratory Tests .....	53
4.1. Boom and Multi-coupling Actuation.....	53
APPENDIX 1 Requirement specification with changelog.....	55

## LIST OF FIGURES

Figure 1 Robominer RM1 autonomous mining robot .....	10
Figure 2 Side view with dimensions and cross-section view .....	11
Figure 3 Module 1 frontal view .....	12
Figure 4 Screw-leg unit .....	12
Figure 5 Lateral cross-section of the boom and the production tool unit .....	13
Figure 6 Boom operation .....	13
Figure 7 Maximum reach of the production tool .....	13
Figure 8 Multi-coupling assembly .....	14
Figure 9 Systems architecture of RM1 .....	14
Figure 10 RM1 with all related systems .....	15
Figure 11 Structural schematic of hydraulic systems .....	16
Figure 12 Hydraulic diagrams of the hydraulic powerpack and water prefiltration unit .....	16
Figure 13 Hydraulic diagrams of Robominer modules 1 and 2. Valve symbols – refer to Figure 14 .....	17
Figure 14 Hydraulic valves in RM1. Top row from left to right: 4 speed 4/3 valve for tool drive control, digital proportional valve for boom and multi-coupling actuators and 4 speed 4/3 valve for screw drive control. Bottom row from left to right: pressure control valve, 3/3 valve and 4/3 valve .....	18
Figure 15 3D-printed mockup of the leg lateral actuator valve block .....	19
Figure 16 RM1 module 1 and module 2 communication system architecture .....	21
Figure 17 RM1 underground station communication architecture .....	21
Figure 18 RM1 ground level communication architecture .....	22
Figure 19 Independent electronic control unit for one screw-leg unit .....	22
Figure 20 Function structure of a pressure reducing valve control .....	23
Figure 21 Circuit diagrams of the valve controller board and pressure reducing valve controller board .....	23
Figure 22 RM1 power delivery system .....	24
Figure 23 Diagrams of auxiliary water supply system and electric supply system .....	24
Figure 24 Water hydraulic 4/3 directional valve .....	25
Figure 26 Water hydraulic servo valve .....	26
Figure 27 150 bar 2/2-valve (left) and 200 bar 2/2-valve (right) .....	26
Figure 28 Direct acting valve test system .....	27
Figure 29 The beginning of the 5 Hz measurement. ....	29
Figure 30 The time value in which the valve stops working .....	29
Figure 31 The pulse ratio as the function of the pwm-signal pulse ratio on the 4 Hz measurement....	30

---

Figure 32 The pulse ratio as the function of the pwm-signal pulse ratio on the 5 Hz measurement....	30
Figure 33 200 bar valve test system .....	31
Figure 34 The beginning of the 2 Hz measurement .....	32
Figure 35 The beginning of the 3 Hz test of the 200 bar valve. ....	32
Figure 36 The real pulse ratio as the function of control pulse ratio with 2 Hz frequency.....	33
Figure 37 Proportional valve built from on/of valves.....	34
Figure 38 Cylinder test bench .....	34
Figure 39 Pulse Density Modulation .....	35
Figure 40 Speed control test with 3 Hz pulse rate in positive direction .....	35
Figure 41 Speed control test with 3 Hz pulse rate in negative direction .....	36
Figure 42 Test with different pulse rates.....	36
Figure 43 Screw internal components on workbench .....	37
Figure 44 Screw internal components in CAD-model .....	37
Figure 46 Screw sled with 200 kg load.....	38
Figure 47 Pull test with bare sled.....	38
Figure 48 Screw sled with 200kg load, pull test with pressure logging .....	38
Figure 49 Pull test with 200kg of load on the sled .....	39
Figure 50 Screw motor pressures when rotating freely in air.....	39
Figure 51 Screw motor pressures when running with no extra load.....	40
Figure 52 Pull force on a plywood surface .....	40
Figure 53 Hydraulic muscle test rig and its hydraulic diagram .....	41
Figure 54 Hysteresis and time dependence in force vs displacement curve of a HAM .....	42
Figure 55 Measured force and modelled force at 6 bar operating pressure .....	42
Figure 56 700 bar pressure chamber.....	43
Figure 57 Pressure cycling test system.....	44
Figure 58 Lithium battery cell after pressurized in oil.....	44
Figure 59 Pressure dependence of different temperature sensors .....	45
Figure 60 Valve controller board .....	47
Figure 61 Pressure regulator circuit board and hydraulic diagram .....	47
Figure 62 Pressure regulator test setup .....	48
Figure 63 Pressure regulator with static flowrate.....	48
Figure 64 Pressure regulator with on/off load .....	49
Figure 65 Pressure regulator with biased on/off load.....	49

Figure 66 Pressure sensor circuit boards and completed sensors..... 50

Figure 67 Reference sensor and new experimental sensor comparison..... 50

Figure 68 Magnet mounted on a servo motor and the sensor..... 51

Figure 69 Protective sensor enclosure ..... 51

Figure 70 Communication network test setup ..... 52

Figure 71 Boom assembly ..... 53

Figure 72 Positioning accuracy test with small steps ..... 53

Figure 73 Path follow test data shifted by 1.2 seconds..... 54

## LIST OF TABLES

Table 1 Test results of the direct acting 150 bar valve.....	27
Table 2 Test results of the 200 bar valve .....	31
Table 3 List of component types and packages pressurized to 50 MPa as a part of a functioning single-board computer. ....	46

## 1. INTRODUCTION

This deliverable document presents laboratory tests performed for certain key components of Robominer autonomous mining robot (Figure 1) which is being developed in ROBOMINERS -project. The robot concept has been introduced in two previous deliverable D3.1 System requirements and D3.2 Robominer design report.

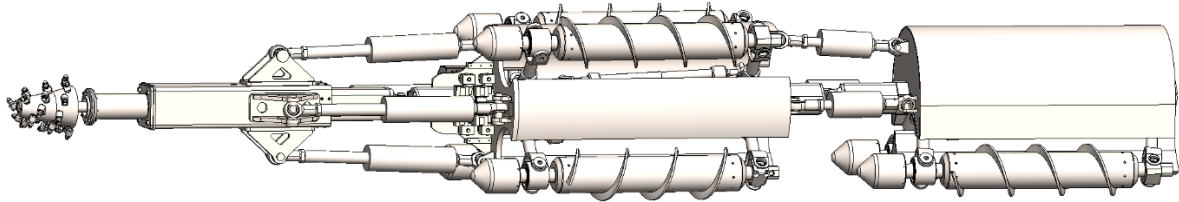


Figure 1 Robominer RM1 autonomous mining robot

During the development process numerous design changes were made in order meet the development targets as closely as possible with the technology available currently. Also, component and material supply challenges caused first by Covid-crisis and later by Russian attack to Ukraine have caused some changes as well as significant delays. These changes and their effects on the robot are analyzed in deliverable document.

Laboratory tests were concentrated in water hydraulics components and electronics which are the areas with biggest development challenges, and which unluckily also have been the areas most affected by two ongoing crises. Electronic component availability issues have affected on the electronics development and forced make design changes. Water hydraulic system development has been affected by stainless steel availability issues and rapid as well as steep increase of its price.

## 2. ROBOMINER PROTOTYPE RM1

### 2.1. Design changes to RM1 during the development in WP3

During the development and design phase some design changes to original concept, introduced in D3.1 and D3.2, were introduced. These changes and their effect on RM1 functions and capabilities are presented in a changelog based on RM1 requirement specification tables in Appendix 1.

### 2.2. RM1 structure and dimensions

Main difference to D3.1 and D3.2 is a change to two module system in RM1. D3.1 and D3.2 envisioned only one module RM1.

RM1 is separated into two modules to increase its traction capabilities and to increase the weight, which is needed to counteract the forces produced by the production tool and the weight of the production tool and the boom. Furthermore, change enables better studying the modular structure and its operation and capabilities in real operational environment. The first and the second module have same dimensions and share the same system component design, but their structural design is different. Main difference in structural design is module 2 having only two screw traction units. The second module has higher volume which gives more room for the system components. Boom and multi-coupling designs are very close to each other to give them similar characteristics and by that to get possibility to study modular configuration and scalability.

Figure 2 and Figure 3 show RM1 final structural design and its main dimensions.

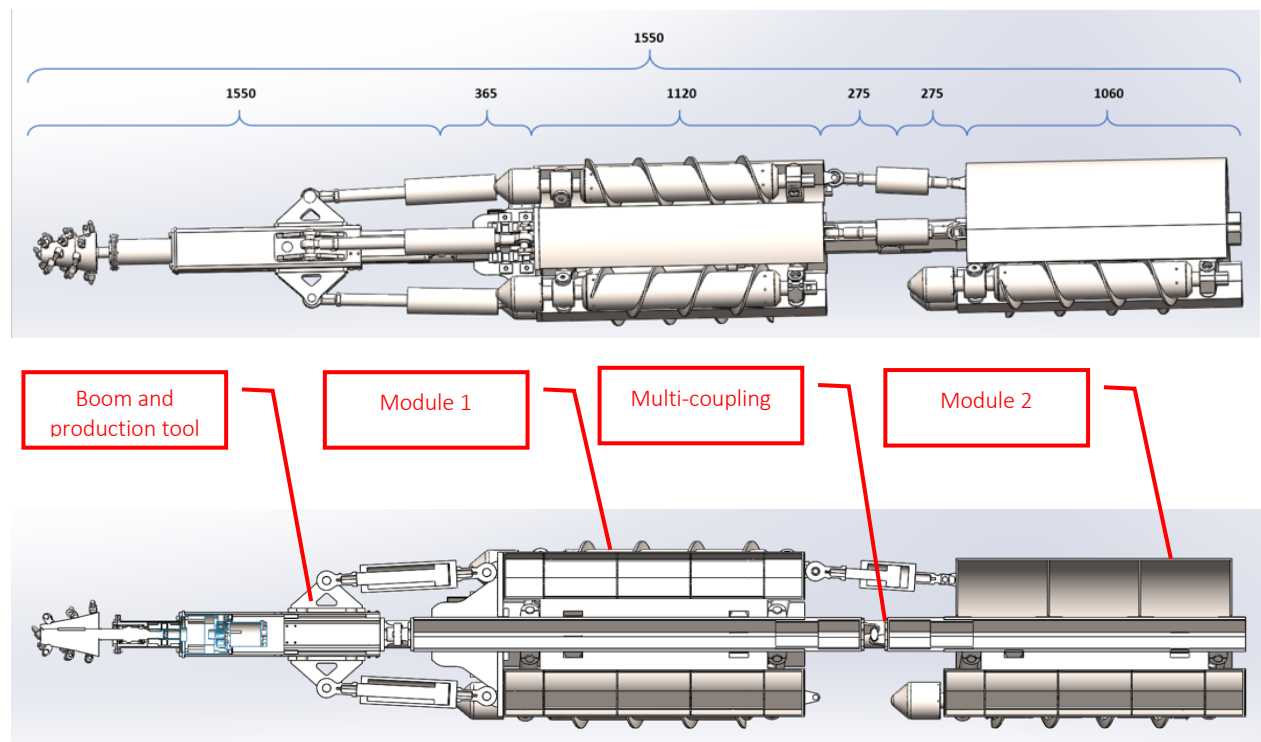


Figure 2 Side view with dimensions and cross-section view

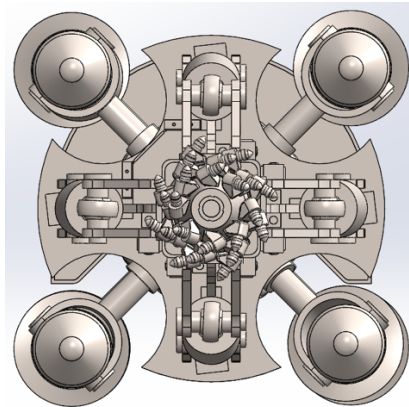


Figure 3 Module 1 frontal view

Screw-leg units (four in module 1 and two in module 2) consist of traction screw (1), inside of which are the water hydraulic screw drive unit, leg radial actuators (2) and leg lateral actuators (3). Radial actuators have a stroke of 70 mm and they can be tilted 30 deg by using lateral leg actuators. All actuators can be controlled independently which gives robot possibility to adjust screw angle to match the terrain and perform rudimentary walking. Figure 4 illustrates the structure of the screw traction unit.

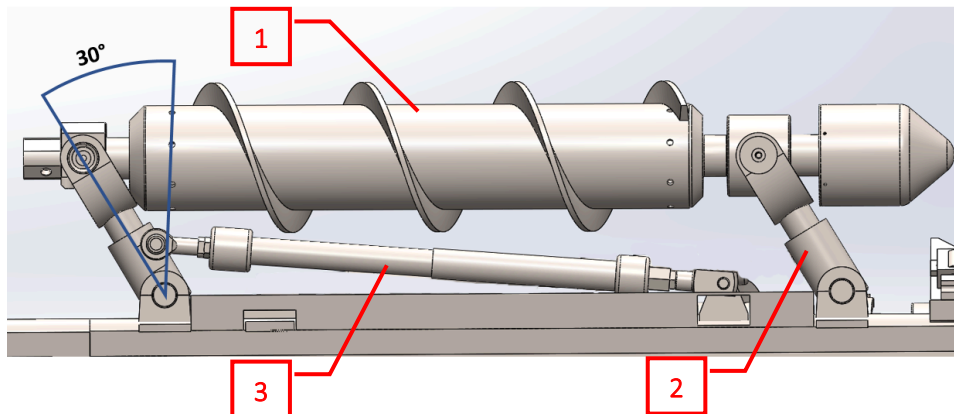


Figure 4 Screw-leg unit

Figure 5 shows a cross-sectional view of the boom and production tool unit. Boom is attached to the body module by a 2-DOF joint (universal joint) (1). The third degree of freedom comes from the telescopic boom (2). The operation principle of the boom is simplified 3-DOF Stewart platform. The four-cylinder solution is chosen instead of three to make force and vibration load distributed more evenly with symmetry. The three-cylinder solution requires usage of a bigger cylinder bore diameter. Bigger cylinders would require stronger eyelet bearings which are not available off the shelf as components which would be structurally suitable. The four water hydraulic actuators (3) solution presents an over actuation problem: 1<sup>st</sup> cylinder defines longitudinal angle, 2<sup>nd</sup> length of the telescope, 3<sup>rd</sup> vertical angle and 4<sup>th</sup> causes over actuation. The problem is handled by the control valves that allow compliance when needed. This is done by including a hydraulic accumulator is included in valve control to compensate control error. The hydraulic cylinders can also be temporarily turned to be forceless if needed. The cylinders are connected to the body and to the boom with 2-DOF rod end bearing. Production tool consists of the water hydraulic production tool drive unit and the cutting head (4).



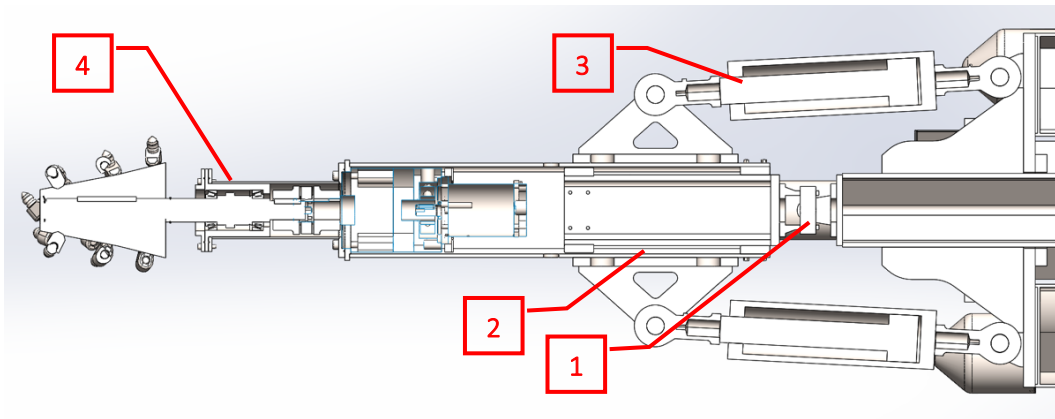


Figure 5 Lateral cross-section of the boom and the production tool unit

Operation principle of the boom is illustrated in the Figure 6, which shows the boom in three positions: Vertical position fully retracted (A), vertical position fully extended (B) and maximum angle fully extended (C). Figure 7 shows the maximum reach of the production tool.

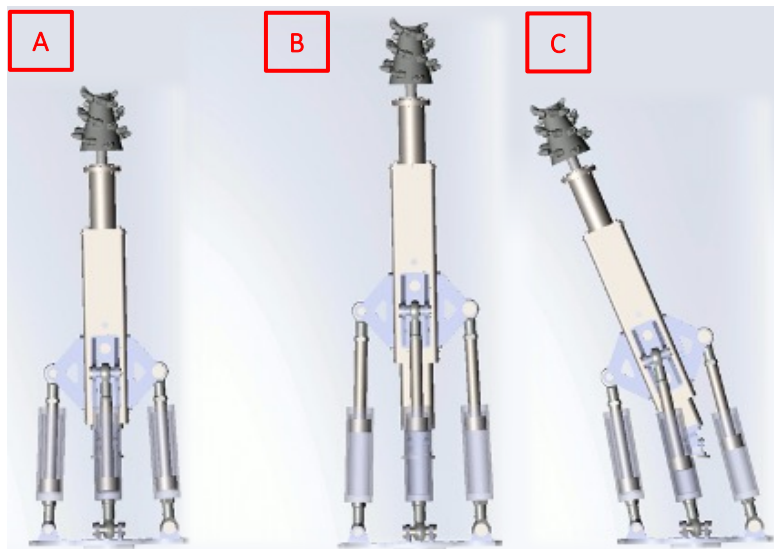


Figure 6 Boom operation

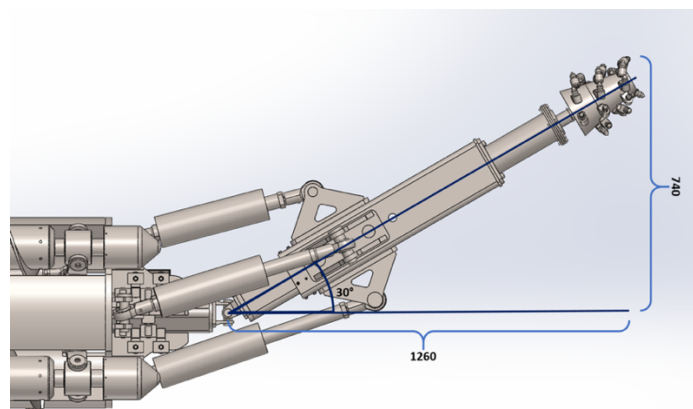


Figure 7 Maximum reach of the production tool

Multi-coupling provides the RMS1 articulated steering and also possibility to worm-like movement by extending and retracting the coupling. It is structurally almost similar to the boom with only exception of having three hydraulic actuators (Figure 8). The fourth actuator is removed to make room for hoses and wires, which are necessary in the prototype, connecting the module 1 and module 2. This effects on the maximum force, but the force is estimated to be adequate for the function of the coupling.

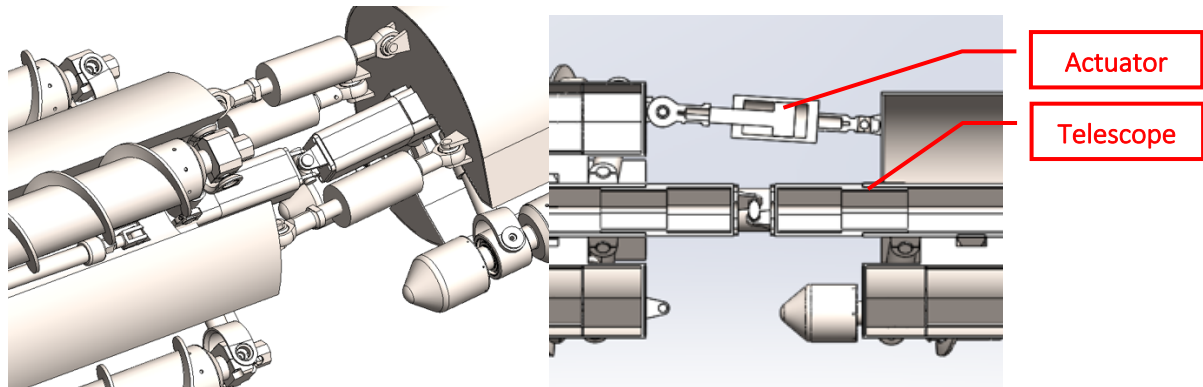


Figure 8 Multi-coupling assembly

Multi-coupling can be either floating, i.e. control valves connect actuator chambers together and the actuator provides only damping, or fully active.

### 2.3.RM1 Subsystems

Systems architecture of RM1 divides the robot in subsystems. Systems architecture of RM1 is presented in the Figure 9.

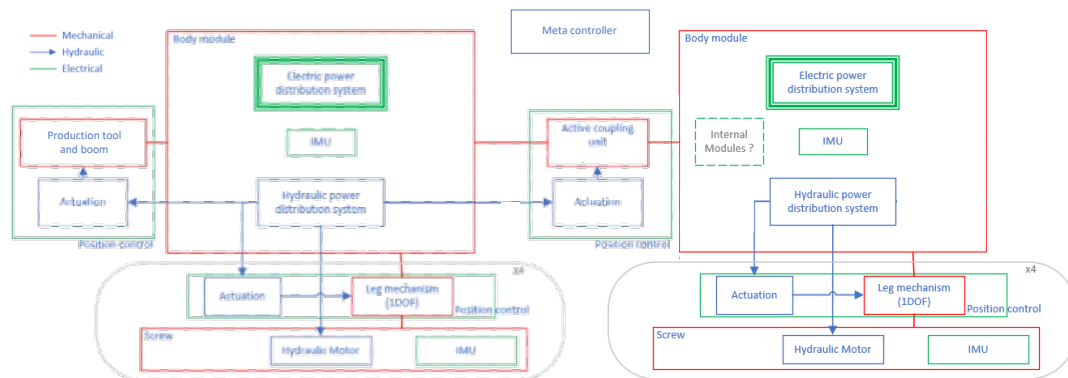


Figure 9 Systems architecture of RM1

The architecture divides RM1 subsystems into logical distributed system entities. Architecture enables robust and reliable subsystem designs by separating different subsystems and functions. Architectural level separation of functions in RM1 on the other hand makes it high level of integration possible.

RM1 has four main subsystems:

1. Hydraulic system
2. Low level control system
3. Power system
4. Auxiliary systems

RM1 with all related systems form a modular system presented in Figure 10. RM1 connects to underground station via the tether which consists of high and low pressure water lines, communications cable, electric supply cable (24VDC) and cuttings transport line. In underground station tether is separated to different lines towards hydraulic powerpack, ground control station and auxiliary water supply. Cuttings are transported only to this point. Ground control station supplies electric power (400VAC) to all systems using it and acts as communications hub. Command and control station (C2) is control and monitoring room.

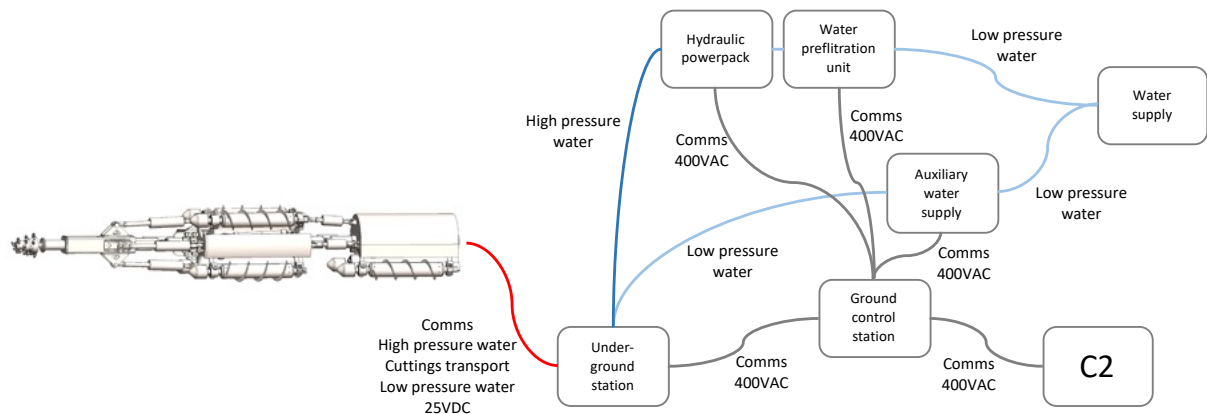


Figure 10 RM1 with all related systems

### 2.3.1. Hydraulic system

Hydraulic system consists of the water hydraulic powerpack, water prefiltration unit, which is needed to ensure the feed water quality, and hydraulic powertrains in RM1 module 1 and module 2. Structural schematic of the hydraulic systems is shown in Figure 11. Hydraulic powertrain main parts are:

- Boom and production tool (1 – Figure 13)
- Screw-leg-locomotion-units (2 and 4 – Figure 13)
- Multi coupling (3 – Figure 13)

The water hydraulic powerpack has the power of 30 kW, maximum flow of 87 l/min and maximum pressure of 160 bar. It is used for powering all RM1 actuators, production tool and screw traction units. Water hydraulic system is a semi-open loop system, which means it recirculates flow back to the powerpack only partly. The remaining return flow is used for flushing dirt sensitive parts of RM1. Hydraulics therefore need continuous supply of water which is fed through the water supply prefiltration unit. Prefiltration unit also works as buffer tank in the water supply. (Figure 12)

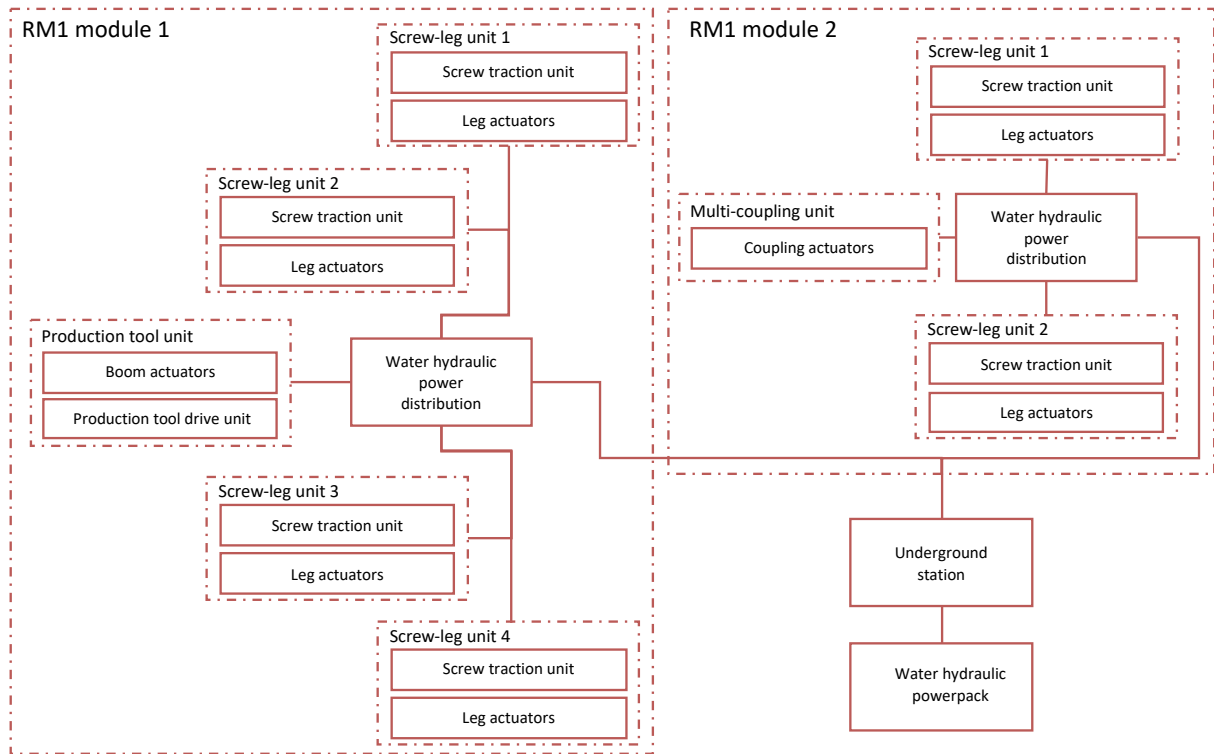


Figure 11 Structural schematic of hydraulic systems

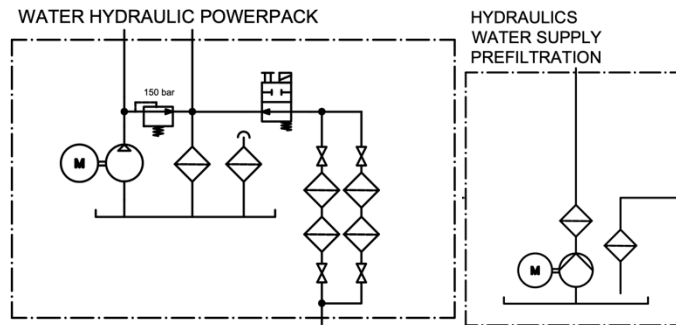


Figure 12 Hydraulic diagrams of the hydraulic powerpack and water prefiltration unit

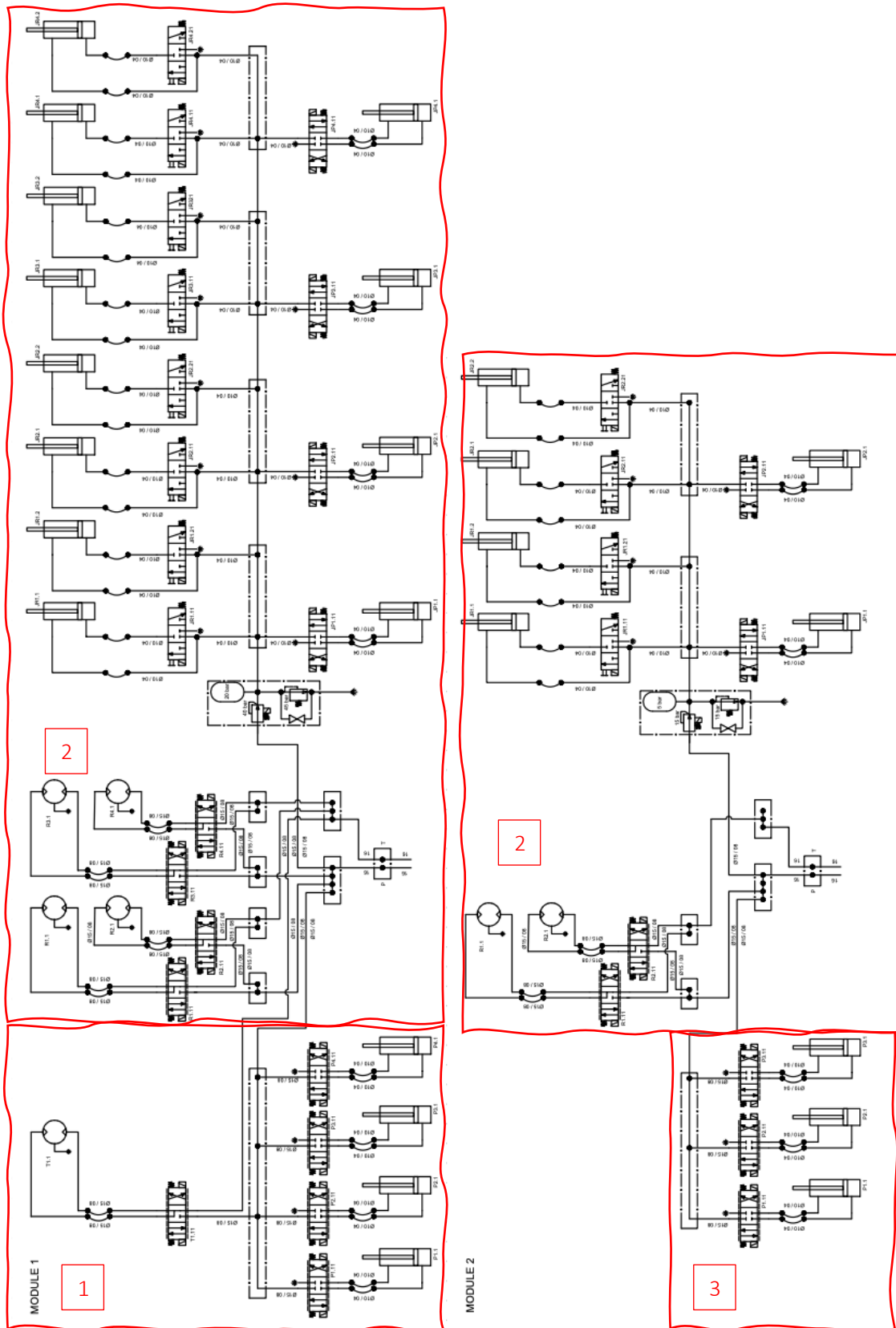


Figure 13 Hydraulic diagrams of Robominer modules 1 and 2. Valve symbols – refer to Figure 14

Hydraulic systems of module 1 and module 2 consist of hydraulic actuators and drive units and their control valves. Functions of hydraulic system are presented in Figure 13. System structure is modular. Actuators and drives have their own control valve blocks which are located near to actuators. The system uses powerpack pressure in all high power actuators, but leg motion actuators use reduced pressure because of high bending forces on the cylinders require big cylinder rods, therefore full powerpack pressure would create too high forces for the mechanism. The pressure reduction valve and related cylinders can be seen in 2– Figure 13.

Due to low availability of COTS valves, especially proportional and servovalves, for water hydraulics, and their generally big size and vulnerability to contamination most of the valves in RM1 are constructed from industrial high pressure water poppet valves. The only exception is the 4/3 directional control valve used in screw drive unit for which a suitable COTS valve was available. Servo controls, i.e. boom and multi-coupling positioning, utilize so-called digital hydraulic control principle. In digital hydraulic control analogue servovalves are replaced by a set of small 2/2 on/off valves which are controlled intelligently to create variable volumetric flow. Valves are also constructed as flexible small volume valve blocks which can fit into RM1. Hydraulic diagrams of valve blocks used in RM1 are shown in the Figure 14. Figure 15 present 3D rendering 4/3 valve as an example of valve block.

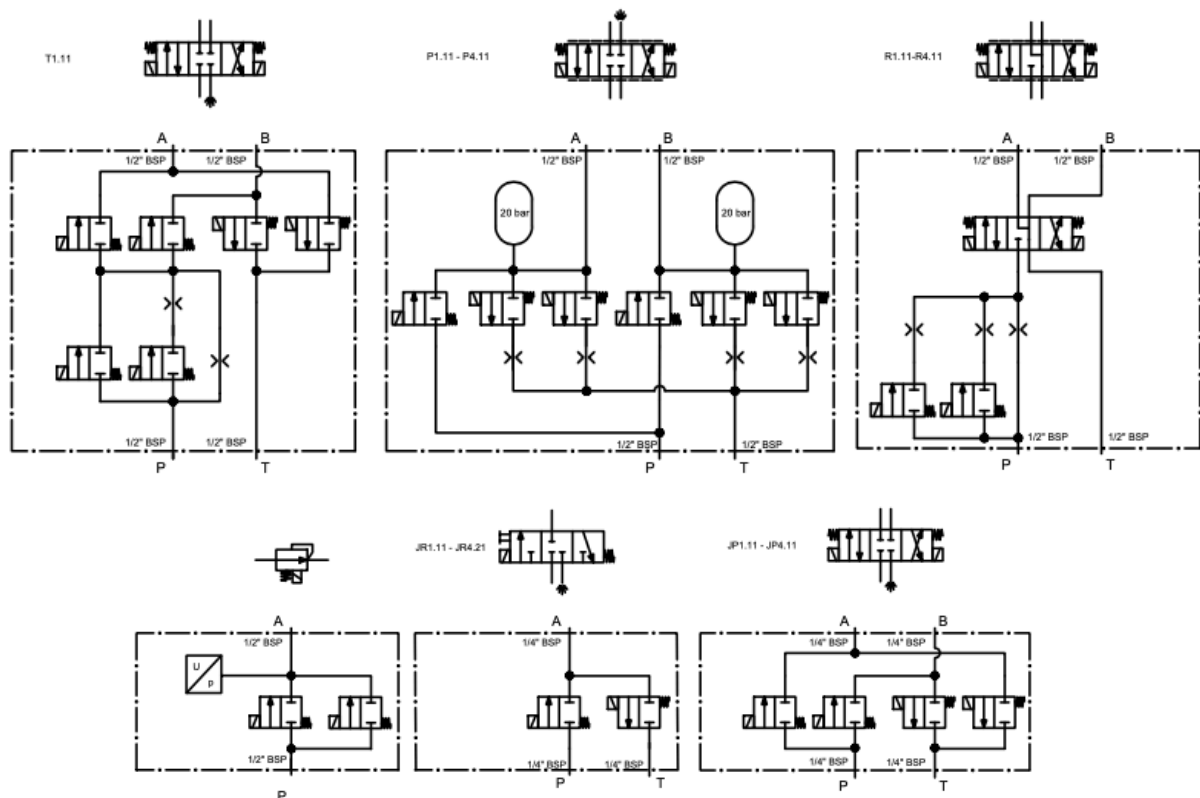


Figure 14 Hydraulic valves in RM1. Top row from left to right: 4 speed 4/3 valve for tool drive control, digital proportional valve for boom and multi-coupling actuators and 4 speed 4/3 valve for screw drive control. Bottom row from left to right: pressure control valve, 3/3 valve and 4/3 valve

Constructing water hydraulic valves from 2/2 poppet valves possesses some definite benefits over more traditional types of hydraulic valves such as spool valves:

- Lower sensitivity to contamination

- Higher damage tolerance due to separately actuated throttling edges
- Individual control of throttling edges, i.e. all possible spool configurations of a spool valve in one valve and change spool configuration during the operation
- Possibility to flow digital control
- Fewer types of valves needed because all valves can be constructed from couple of types of 2/2-valves

However, there are also drawbacks:

- More complicated control electronics
- High level of integration requires complicated valve blocks

It must also be noted that usage of industrial high pressure water 2/2 poppet valves is only a solution applicable to the prototype. Valves are not designed for this purpose and their lifetime in valve blocks controlled with high frequency digital control can be limited due to mechanical wear and fatigue of the spring. Limited lifetime in prototype is acceptable and can be dealt with, but industrial product would need purpose designed 2/2-valves (currently unavailable as COTS components). Purpose designed valves would also reduce the size of valve blocks and improve their performance.



Figure 15 3D-printed mockup of the leg lateral actuator valve block

Figure 15 shows a 3D-printed mockup of leg lateral actuator valve block with real 2/2 valves. Comparison to commercial valve with comparable characteristics shown in the Figure 24 shows that there is no there is no benefits in actual valve volume and weight. However, as can be seen in Figure 14, this valve can offer all possible spool configurations within one valve, which makes it possible to for example select between floating centre position or fully closed and everything in between. Furthermore, having separately controlled throttling edges increases the damage tolerance of the valve. Furthermore, as valve block is purpose designed the directions and sizes of valve ports can be freely selected, which is of an utmost importance because hydraulic pipes and hoses will take a big share of the space inside RM1 and connecting them the way which saves space will free space for other components and systems.

Hydraulic muscles were envisioned to be used as linear actuators in D3.2 because of their robustness and favourable controllability. It however became evident during the development that muscles cannot



provide forces high enough to handle forces created by the production tool. Thus, muscles are replaced by conventional hydraulic cylinders. Muscles, however, can provide a favourable alternative once the high pressure muscles finally become available as COTS components.

### 2.3.2. Low level control and communications systems

Robominer low level control system is developed to be pressure tolerant, i.e work under water in ambient pressure to hundreds of meters of depth in light pressure compensated enclosures. Control system, consists of:

- Valve controllers with embedded control software
- Pressure and position sensors
- ROS2 nodes and interfaces

Robominer communication system consists of:

- Internal robot communication network
- Tether connecting the robot to the underground station
- Underground station
- Tether connecting the underground station to the ground control and monitoring station
- Ground level system

The tether is based on fiber optic technology and internal communications is based on wired ethernet technology. The electric signal is converted to the optic at the ground level connection point. At the underground connection point, optic signal is converted to electric and back to optic before leaving towards the robot. In the first robot module, it is converted to electric again and distributed inside the module and to the second module.

Communication system architecture is illustrated in Figure 16, Figure 17 and Figure 18. Figures show the architecture of communication system inside the robot, in underground station and in ground level.



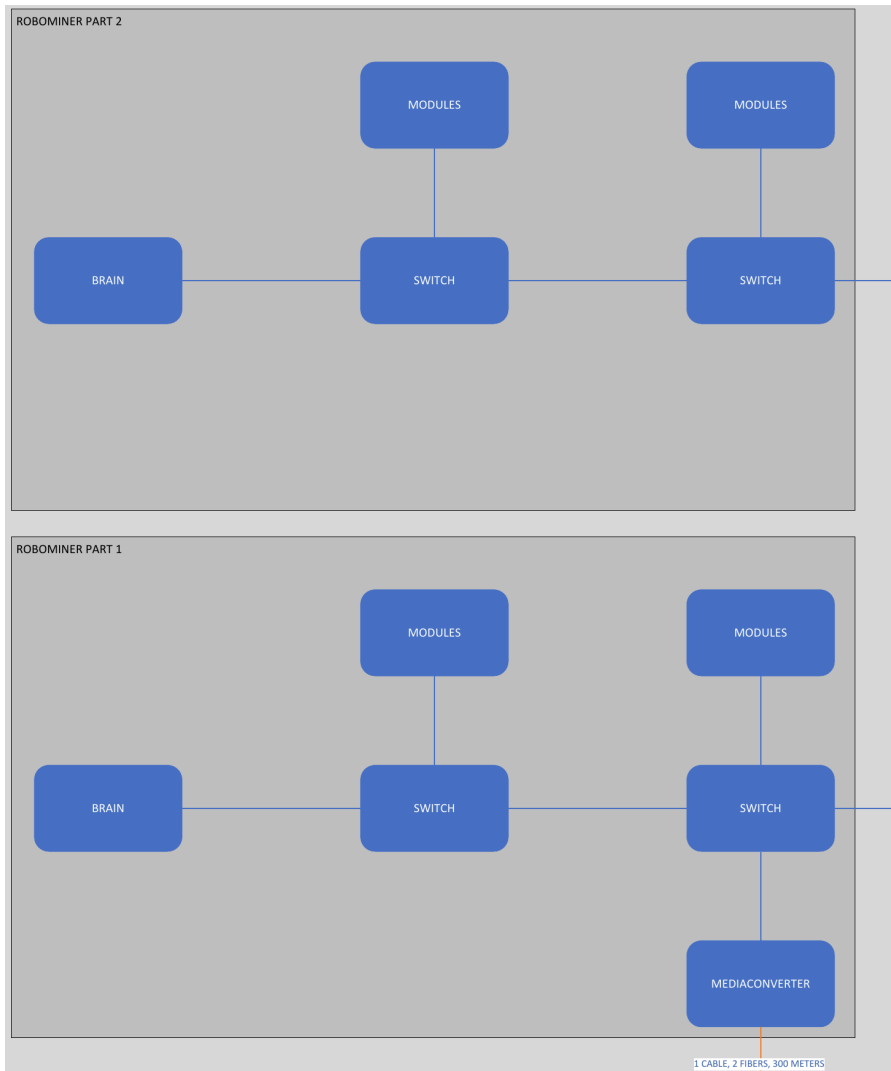


Figure 16 RM1 module 1 and module 2 communication system architecture

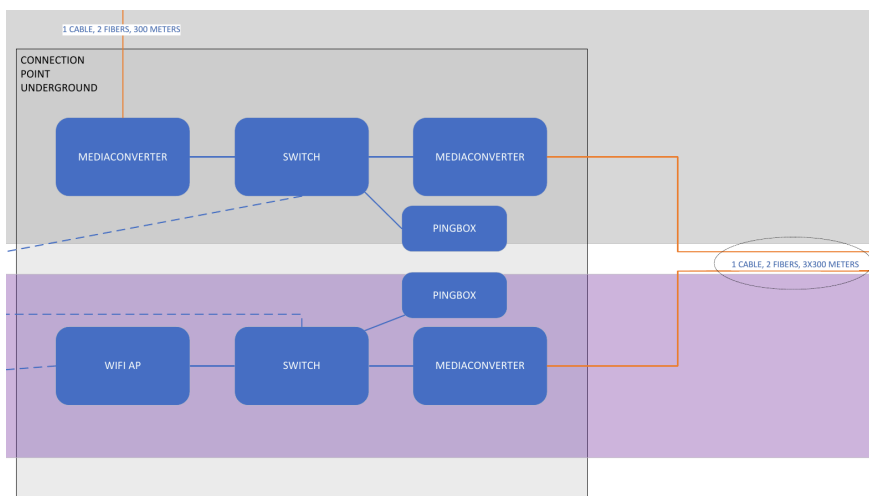


Figure 17 RM1 underground station communication architecture

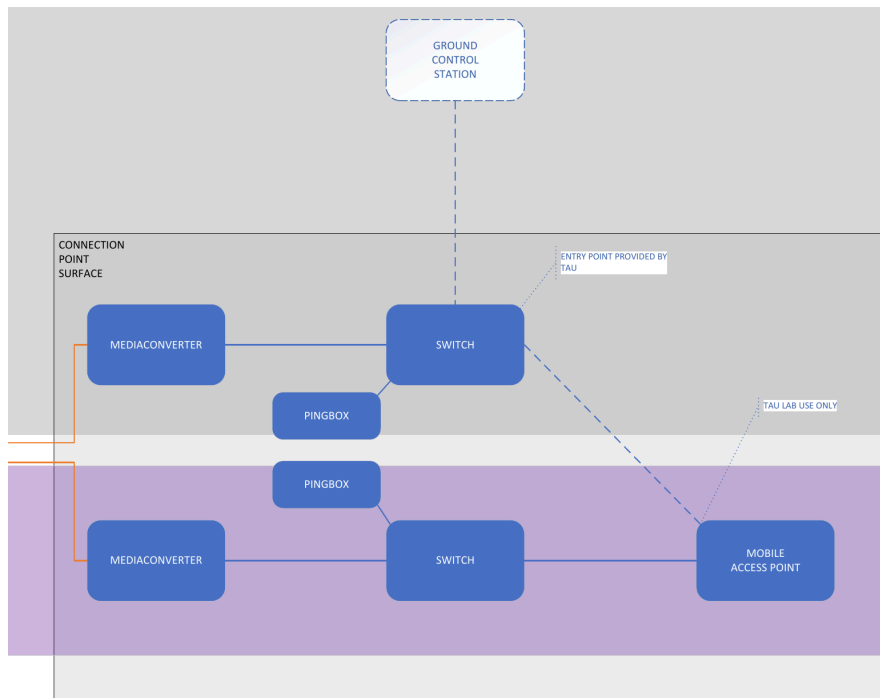


Figure 18 RM1 ground level communication architecture

Independent electronic control units control actuations and drives in RM1. Control units contain SBC (Olimex A64-OLinuXino) and micro controller (Raspberry Pico) for computing and communications and thus they are in the point of view of the higher-level control individual ROS-nodes. One board can control 16 solenoids and it can read simultaneously 8 analog inputs. In addition, 4 position sensors can be read via SENT-bus. Wired Ethernet is used for communication with higher level control system. They also include self-monitoring functions to monitor both electronics in them and the related hydraulic circuit. Functional structure of a control unit (valve controller) for one screw-leg unit is shown in the Figure 19.

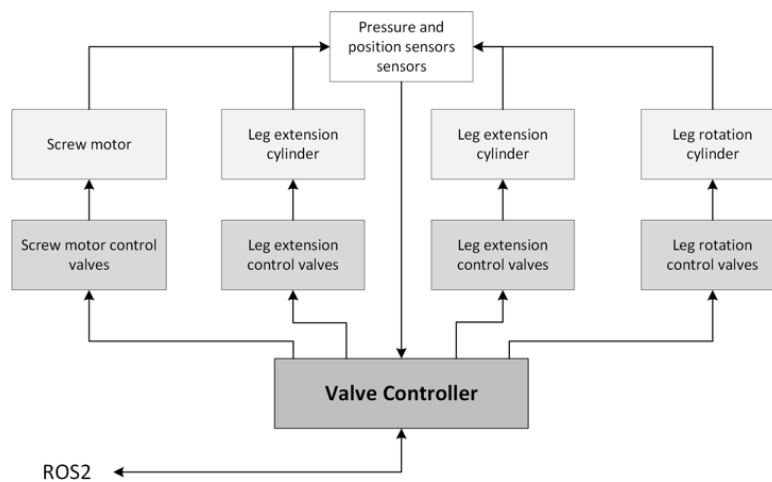


Figure 19 Independent electronic control unit for one screw-leg unit

Function structure of pressure reducing valve is shown in the Figure 20.

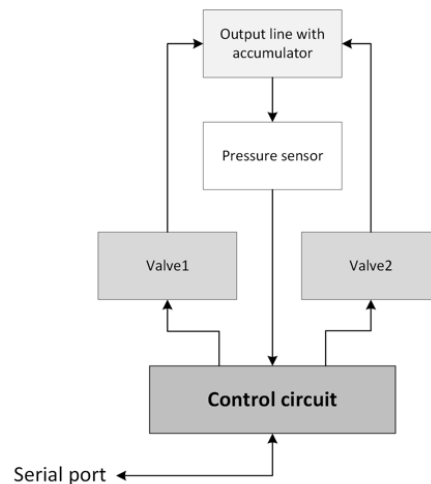


Figure 20 Function structure of a pressure reducing valve control

All actuators and drives can be controlled with one type of the electronic control unit (valve controller) shown in the Figure 21. Another type of electronic control unit was developed for pressure reducing valve control (Figure 21). Pressure reducing valve controller board uses a microcontroller instead of SBC because it has less inputs and outputs, and computational requirements are not high. Board controls two 2/2 on/off valves in closed loop on the basis pressure command and pressure feedback.

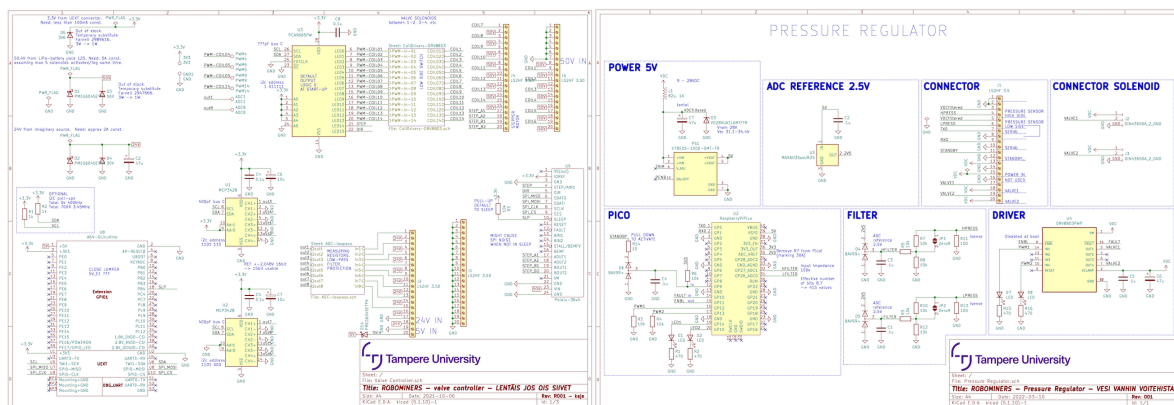


Figure 21 Circuit diagrams of the valve controller board and pressure reducing valve controller board

### 2.3.3. Power system

Electric power system (Figure 22) is based on 24 VDC power supply tether and internal batteries, which are used to provide peak power to robot's internal managed microgrid. Battery pack is 6 cell lithium-polymer construction with the capacity of 20 Ah.

Design changes to suggested solutions of D3.2 were made due to global component shortage. Component shortage caused that it is not possible to build the envisioned microgrid management system. Still, different power consumers are protected separately for over current and over voltage.

In D3.2 voltage was defined to 48 VDC but is changed to other common voltage of 24 VDC. This decreases number of power supplies and is possible to construct while challenges to obtain components persists. The battery management system is responsible only for cell balancing as the power feed from underground station is current limited by the power supply and by the resistance of

the tether. Microgrid management will be realized using commercial battery and power management hardware.

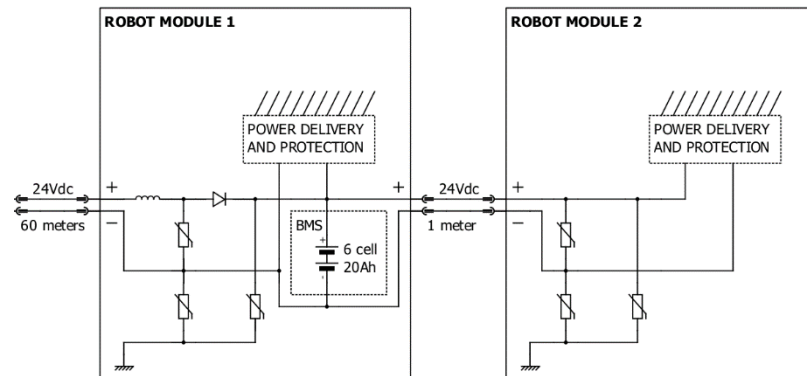


Figure 22 RM1 power delivery system

### 2.3.4. Auxiliary systems

Auxiliary systems development was finalized. Auxiliary systems of RM1 are the ground support systems, which include auxiliary water supply for cutting and material transport and electric supply system (Figure 23). Auxiliary water supply system consists of a centrifugal pump (size to be defined), buffer tank and strainer for incoming water. Electric supply system consists of two electrical centres: Ground control station and underground station. Electricity (400 VAC, 3 -phase, 100 A) is supplied to underground station where it is transformed to 24 VDC which is supplied to RM1 via tether and further supplied to ground control station (400 VAC, 3 -phase, 16 A). Both stations have individual UPS-units to guarantee continuous supply in case of power failures.

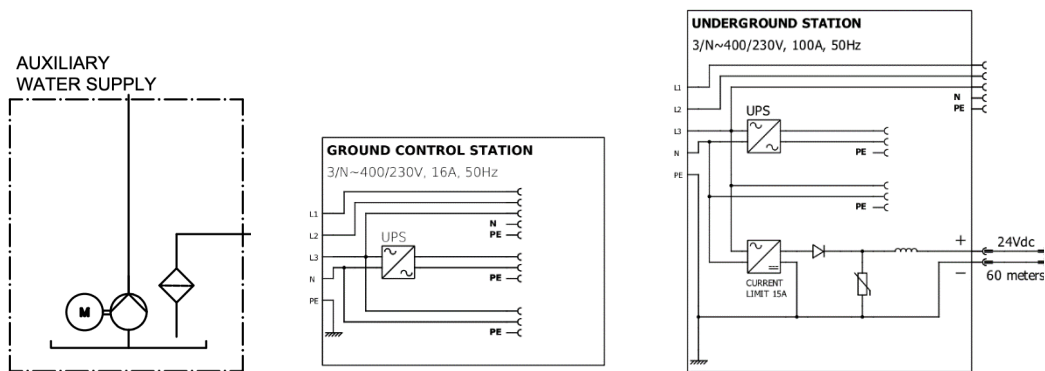


Figure 23 Diagrams of auxiliary water supply system and electric supply system

### 3. COMPONENT AND SUBSYSTEMS LABORATORY TESTS

Powertrain laboratory tests were conducted to:

- Individual 2/2-valves used in valve assemblies to study their dynamics
- Control and pressure reducing valve assemblies to study their performance
- Traction screws to study their performance
- Hydraulic muscles

Sensors and electronic components and systems were tested both for their functionality and performance and their pressure tolerance. Functionality and performance were tested in powertrain laboratory tests, which all were done using the real control hardware and embedded software. Pressure tolerance tests were performed in pressure chamber developed for the purpose.

#### 3.1. Water Hydraulics Components

##### 3.1.1. Water Hydraulic 4/3-Valves

The hydraulic schematic contains many 4/3 type valves, but the COTS options are limited; only feasible options are directional control valve and servo valve from The Water Hydraulics Company. However, these valves have very low flow capabilities, very high cost, and relatively big physical size. The on/off acting directional control valve has nominal flow rate of 30l/min at a pressure loss of 35bar. The big physical size of this valve makes it less sensible to use in leg control than a combined set of small 2/2 valves, and the low flow rate and on/off behaviour makes it less ideal for traction screw unit control; it requires a separate flow control valve to have control over speed of the traction screws. To optimize use of space this directional valve is intended to be used for the traction screws, as making the same flowrate with 2/2 valves requires use of bigger 2/2 valves and that would make a bigger assembly than this valve. In case of traction screws the drawback of high pressure loss is not critical, it just limits the maximum force at full speed. This is seen unacceptable in the case of production tool, and there a digital speed control block is to be used instead of 4/3 valve.

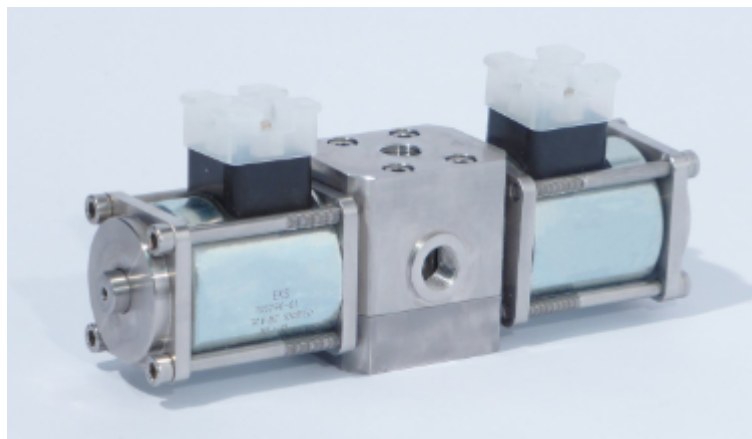


Figure 24 Water hydraulic 4/3 directional valve

The only available COTS flow control valve is a servo valve of similar construction, but with significantly greater pressure loss. The servo valve is specified to 27l/min at a differential pressure of 100 bar, which is two thirds of the system pressure. Realistically the servo can thus only be used in very low flow demanding applications, and such applications in RM1 are only a few. In addition, the servo valves are very expensive, and physically big. The on/off type 2/2 valves are also more robust and dependable and use simpler control than the servo unit. Therefore, the use of different valve types is not seen

reasonable, but the intention is to use valve packs made of small 2/2 valves as such packs will nevertheless be mandatory in most of the actuators.



Figure 25 Water hydraulic servo valve

### 3.1.2. Water Hydraulic 2/2-Valves

Many valve controls in RM1 are based on two 2/2 valve types shown in Figure 4. Valves have different flow capacities: 200 bar pilot operated valve has equivalent orifice size of 8 mm and 150 bar direct acting valve has equivalent orifice size of 1.2 mm. Also, their operation principle differs the first one being pilot operated and the latter direct operated, which has an effect on their dynamics. In typical applications of this type of valves the effect of dynamics is insignificant and therefore manufacturers do not supply nor measure them. However, to use these valves in digital hydraulic servo or proportional controls and other controls the minimum requirement is to know maximum control frequency and related characteristics of valves.



Figure 26 150 bar 2/2-valve (left) and 200 bar 2/2-valve (right)

The maximum control frequency was measured for both valves. The 150 bar direct acting valve was tested with the maximum flow of 7-8 l/min. The diagram of the test system for the valve is shown in Figure 27.

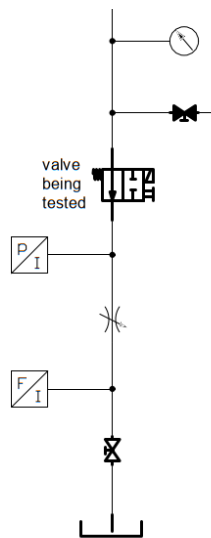


Figure 27 Direct acting valve test system

A valve controller board (Chapter 3.2.2) was used to control the valve being tested and to acquire measurement data. The sampling frequency on the measurements was 100 Hz. The measurements were conducted as duty cycle sweeps, i.e., varying the time which the valve is open divided by the time the valve is closed during one pwm-pulse. The duty cycle is a percentage value in the range of 0-100%. In the measurements the initial duty cycle was 0% and it was increased evenly to 100%. The duty cycle sweeps were used in the test since it is beneficial to know the duty cycle control range with a certain frequency.

Every measurement was started with calibration. In the calibration the valve was open, and the throttle valve was adjusted so that the pressure after the valve was set to 11 bars to see the opening of the valve clearly on the results. The pressure after the valve was set low to decrease the effect of compressibility. The pressure before the valve and the water flow were measured in the beginning of the measurement during the calibration. The voltage used in the measurements was chosen to be maximum recommended by the manufacturer (24 V) to get the maximum force out of the valve solenoid.

The results of measurements are in the Table 1. The frequency for the first measurement were set to 2 Hz. The measurement frequency was incremented by 1 Hz to the 15th measurement.

Table 1 Test results of the direct acting 150 bar valve

Measurement	Frequency (Hz)	Voltage (V)	Flow (l/min)	pressure before the valve (bar)	Pressure after the valve (bar)	Pressure over the valve (bar)
1	2	24	1,55	96	11,2	84,8
2	3	24	2,82	95	10,9	84,1

3	4	24	2,04	95	11	84
4	5	24	2,87	96	10,8	85,2
5	6	24	2,19	96	10,9	85,1
6	7	24	1,67	96	11,2	84,8
7	8	24	2,71	96	14,3	81,7
8	9	24	2,15	96	14,5	81,5
9	10	24	1,67	96	14,9	81,1
10	11	24	2,78	96	14,3	81,7
11	12	24	2,15	96	14,5	81,5
12	13	24	1,61	96	14,8	81,2
13	20	24	3,07	96	14,1	81,9
14	14	24	2,25	96	14,5	81,5
15	15	24	1,5	96	15	81

The measurements were stopped to 15 Hz because in the 15 Hz measurement the valve worked only a small time on the beginning and the valve remained open the rest of the time of the measurement as a result of electromagnetic properties of the solenoid.

Studying the results shows that the valve can work only about 75% of the duty cycle sweep time with 6 Hz frequency and it was concluded that the maximum control frequency of the valve must be under 6 Hz. The valve follows the control signal well with 5 Hz frequency. On the picture below the beginning of the 5 Hz test is shown. In the blue pressure curve in the Figure 28 the pressure rises to 10,8 bar which is the maximum pressure after the valve. This means that the valve is fully opened when the pressure signal value is 10,8 bar. It can also be seen that the pressure decreases to about 1 bar which means that the valve is fully closed.



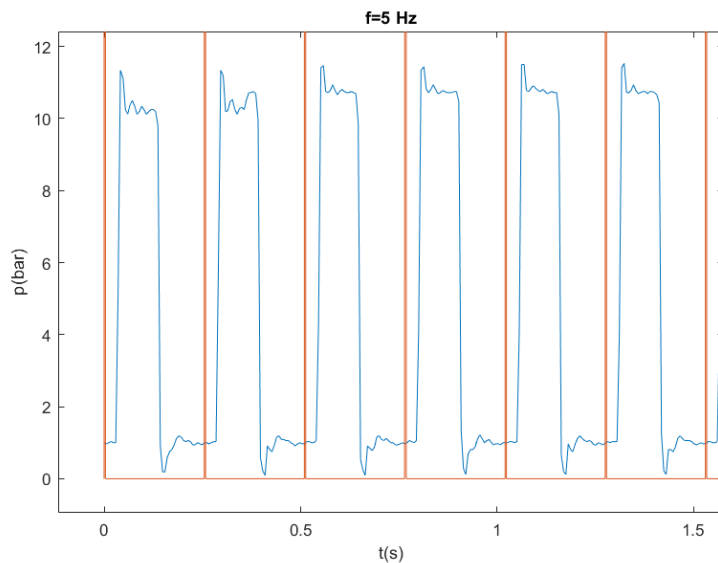


Figure 28 The beginning of the 5 Hz measurement.

After a certain time the valve stopped working which can be seen in the Figure 29. The reason for this is that the valve control signal closing time reached the smallest possible valve closing time. A similar behavior naturally happens in all tested frequencies.

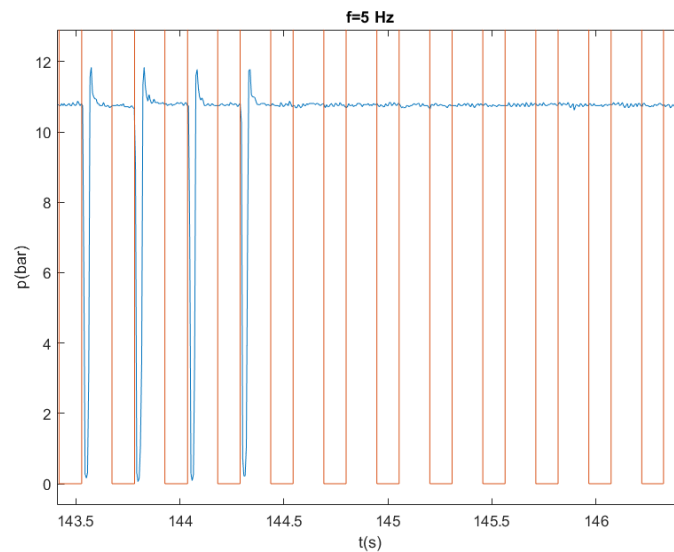


Figure 29 The time value in which the valve stops working.

In order to determine the maximum control frequency providing high enough duty cycle the pulse ratio ranges of the measurements were compared. To compare the pulse ratio ranges the pwm-signal pulse ratio were calculated on 11 different points of the measurements. The points included the start and the end time and 9 time points between them with constant time intervals. The real valve pulse ratios were calculated on the same points from the pressure data.. The pwm-signal pulse ratio and the real valve pulse ratio were illustrated with graphs. The pulse ratio graphs for the 4 Hz and 5 Hz measurements are on the pictures below.

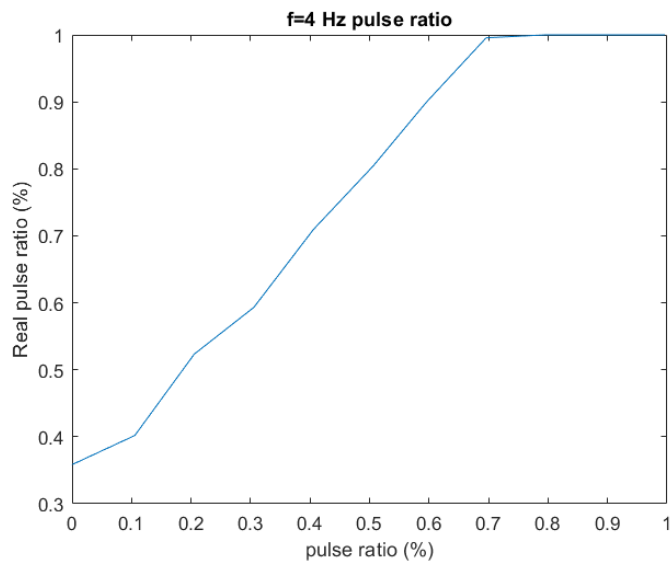


Figure 30 The pulse ratio as the function of the pwm-signal pulse ratio on the 4 Hz measurement.

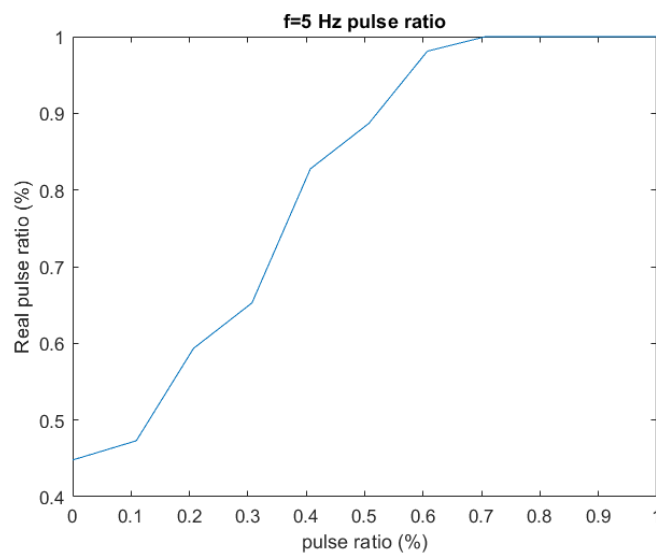


Figure 31 The pulse ratio as the function of the pwm-signal pulse ratio on the 5 Hz measurement.

The valve pulse ratio increases quite linearly in both 4 Hz and 5 Hz measurements. It can be seen from the Figure 30 that with the 4 Hz control frequency that the valve pulse ratio can be controlled from about 36% to 100%. Figure 31 shows that the valve pulse ratio can be modified from about 45% to 100% with 5 Hz control frequency. The pulse ratio control range with 5 Hz was seen to be too narrow for the Robominer application. However, with the 4 Hz control frequency the pulse ratio control range was large enough and therefore the 4 Hz was chosen as the maximum control frequency for the 150 bar valve.

Figure 32 shows the hydraulic diagram of the 200 bar valve test system. The 200 bar valve was tested with the same duty cycle sweeps than the 150 bar valve. The starting frequency was set to 1 Hz and the frequency was increased by 1 Hz in each individual test. The voltage was chosen to be 24 V (the maximum voltage). The water flow was set to 10 l/min. The pressure difference over the valve was kept

constant with only the frequency changing. The reason for this is that the pilot operated valve was estimated to be sensitive to the change of pressure difference over the valve. The water flow, pressure before the valve and pressure after the valve were measured on the calibration in the same way than in the 150 bar valve tests. Below is a table of the test results.

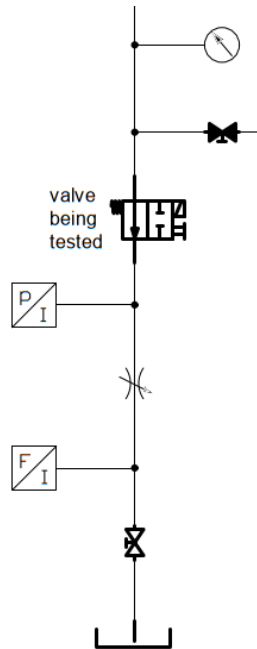


Figure 32 200 bar valve test system

Table 2 Test results of the 200 bar valve

Measurement	Frequency (Hz)	Voltage (V)	Flow (l/min)	Pressure before the valve (bar)	Pressure after the valve (bar)	Pressure over the valve (bar)
1	1	24	9,9	16	12,9	3,1
2	2	24	10,11	16	13,2	2,8
3	3	24	9,93	16	13	3
4	4	24	10,03	20	17	3
5	5	24	9,9	20	17,2	2,8
6	6	24	9,9	20	16,6	3,4
7	7	24	10,12	23	19,8	3,2
8	8	24	10,14	23	19,9	3,1

According to the test results the 200 bar valve can work quite well with 2 Hz control frequency. Figure 33 shows the beginning of the 2 Hz test. In the beginning of the 2 Hz test the pressure decreases to about 1 bar in the pressure pulses which means that the valve closes completely. As for the 150 bar valve also the 200 bar valve remains open after a certain time.

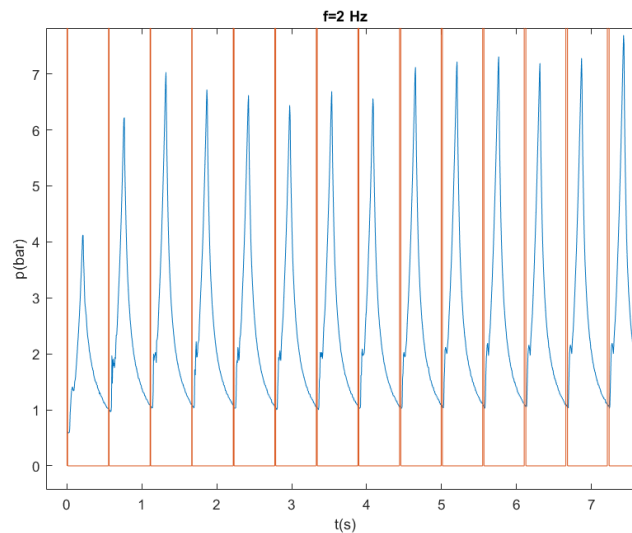


Figure 33 The beginning of the 2 Hz measurement

The beginning of the 3 Hz test is in the Figure 34. It can be seen that the pressure does not anymore decline to about 1 bar pressure. This means that the valve does not close completely with 3 Hz frequency and therefore 2 Hz is the maximum control frequency for the 200 bar valve.

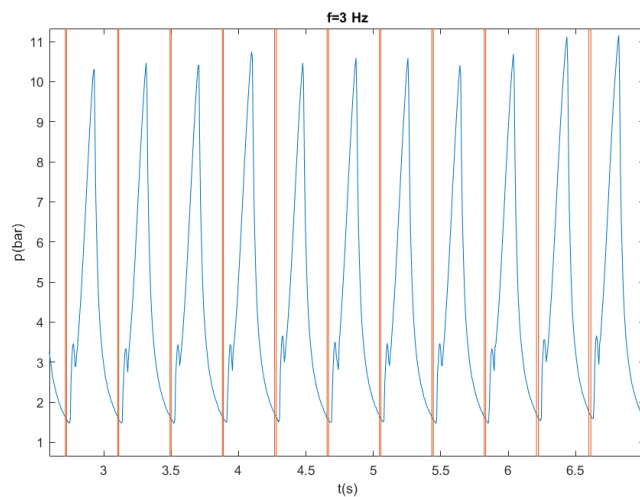


Figure 34 The beginning of the 3 Hz test of the 200 bar valve.

The valve pulse ratio and the control signal pulse ratio were calculated from the data in the same way as for the 150 bar valve. The pulse ratio as a function of the control signal pulse ratio is shown in the Figure 35.

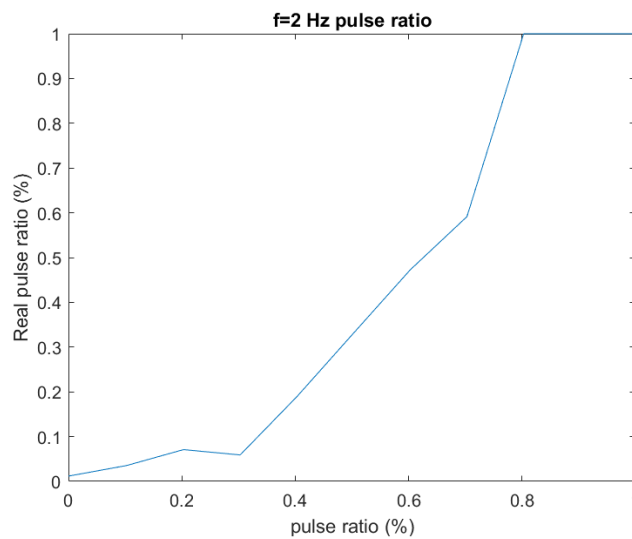


Figure 35 The real pulse ratio as the function of control pulse ratio with 2 Hz frequency.

The tests revealed that PWM control is not suitable for these valves. On higher frequencies PWM suffers from a limited control range. To get a higher range, frequency must be lowered resulting in poor control resolution. The bigger 200 bar pilot operated valve is not suitable for fast switching, but the smaller 150 bar direct acting valve can be used with a different pulse modulation. Usage of Pulse Density Modulation is explored on chapter 3.1.3. The bigger valve will be used with a traditional binary digital hydraulics control scheme to produce different speeds for the screws.

### 3.1.3. Proportional 4-way valve composed of on/off valves

The purpose of this valve assembly is to control both speed and direction of a cylinder on the robot's boom, using simple on/off valves. Typically, this is done with a proportional four-way valve, however selection of suitable off-the-shelf water hydraulic proportional valves is extremely limited or nonexistent. So, the only feasible solution is to use digital control with 2/2-valves. To control flow direction with on/off-valves, they must be arranged similarly to a H-bridge (Figure 36). This configuration allows direction control by opening pressure-line and return-line from opposite sides of the H-bridge. In the test setup valves were connected with fittings which take large amount of space and the complete blocks is bulky. In RM1 valve will be installed as a purpose designed valve block as lack of space inside the robot body is a major concern and it is imperative that space usage is as effective as possible.

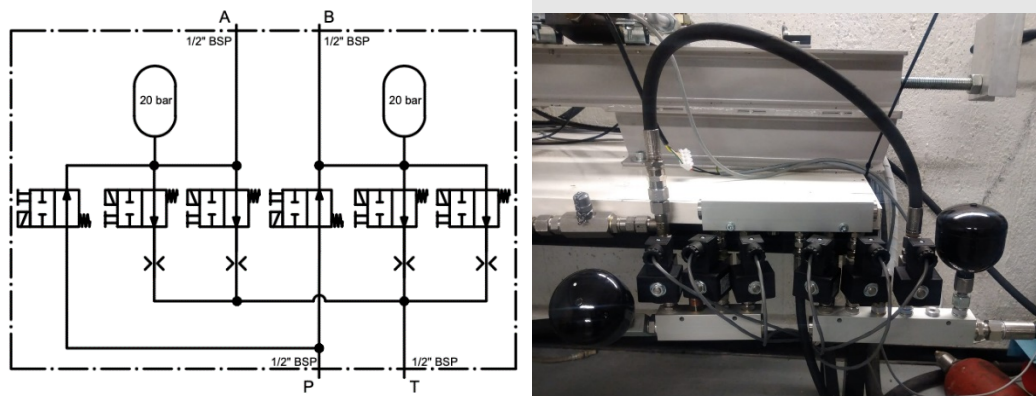


Figure 36 Proportional valve built from on/of valves

This structure allows independent control of both output lines A and B, meaning that it can produce all center position variations of a traditional proportional valve, so it is possible to connect both lines to pressure, to tank or to each other. Flowrate is controlled by rapidly switching the return line valve of a given direction. The valves used are not fast enough to be controlled with Pulse Width Modulation, so Pulse Density Modulation is used instead. Water is let through in pulses and the rate of these pulses determines the relative flowrate. As the valves are slow, two are used to double the rate of pulses and increase control resolution, another benefit is added redundancy. Because the flow is in pulses it causes the actuator to vibrate, hydraulic accumulators are used as low-pass filters to get a smoother behaviour.

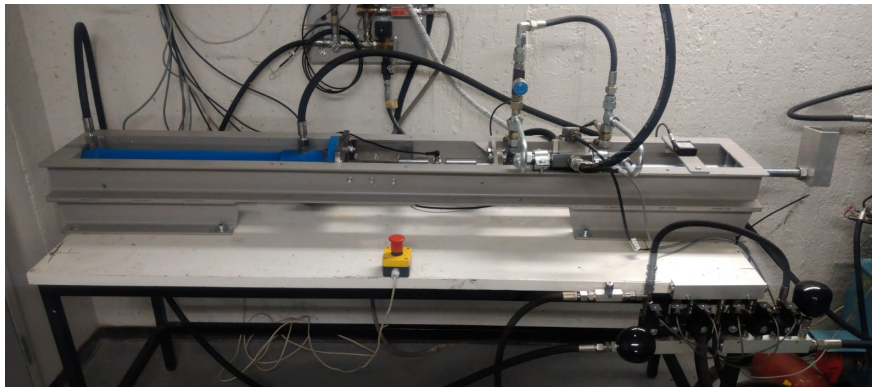


Figure 37 Cylinder test bench

The goal is to use this valve assembly to control the hydraulic cylinders of the production tool manipulator arm/boom. The final dimensions of the cylinders are not yet known, but the one used in these tests is within the same size class. The ability to control a cylinder was tested on a testbench that can produce different loads for the controlled cylinder (Figure 37). The testbench also includes force and distance measurements. Load used in tests was 10000 N push against the water cylinder at 100 bars.

Control loop used is a simple proportional control with a dead zone. The valves are controlled with a Pulse Density Modulation (Figure 38). According to earlier tests the valves have a maximum cycle rate of 15 Hz. At maximum rate the valve takes approximately the same amount of time to open and close and essentially are at 50% duty-cycle. In order to get above 50% duty-cycle the behaviour is flipped to have the valves open by default and being closed at declining rate. This is illustrated in Figure 38.

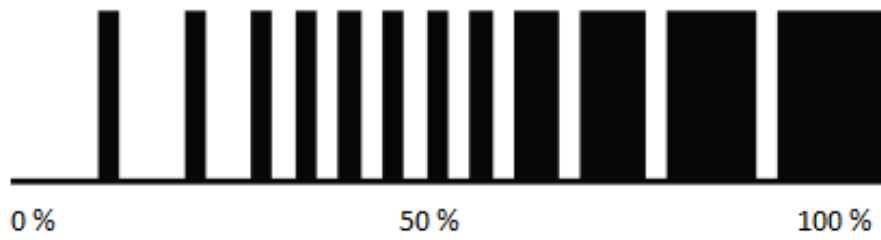


Figure 38 Pulse Density Modulation

Major concern of this type of control valve is that the movement will not be smooth, especially at lower speeds. One pulse creates enough flow to move the cylinder about 2.5 mm and 3 Hz pulse rate creates velocity of 7 - 9 mm/s depending on the direction of movement and load. Figure 39 shows a test with constant pulse rate and resulting position and velocity plots. The position seems to change linearly, but velocity is not smooth.

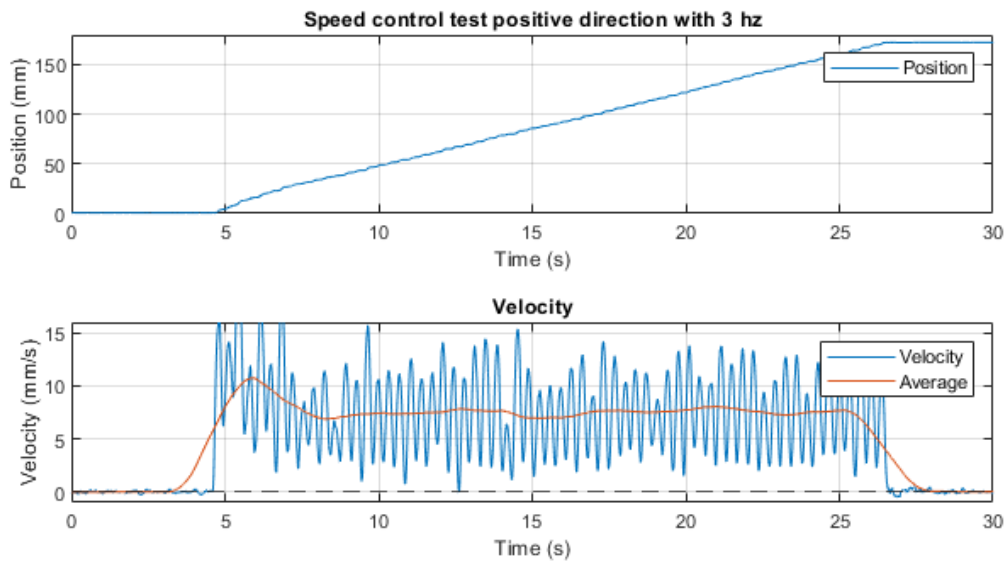


Figure 39 Speed control test with 3 Hz pulse rate in positive direction

In Figure 40 test is ran in the opposite direction and against the load. In this instance, the velocity is much smoother. Even though the movement is against the load, velocity is higher in this direction

because the cylinder area is smaller meaning that the same flowrate will result in higher speed, this can be mitigated by using different orifices in the valves.

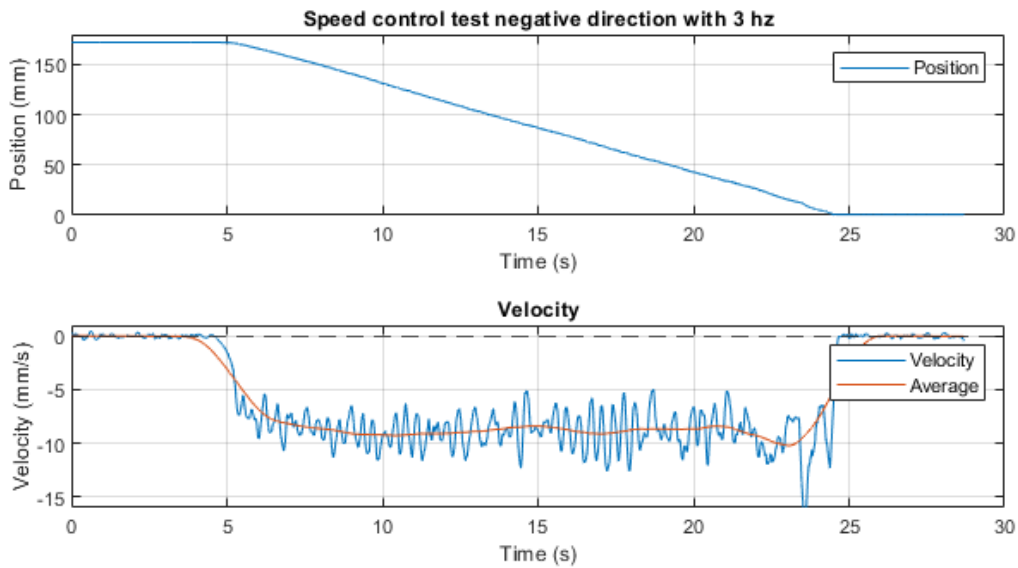


Figure 40 Speed control test with 3 Hz pulse rate in negative direction

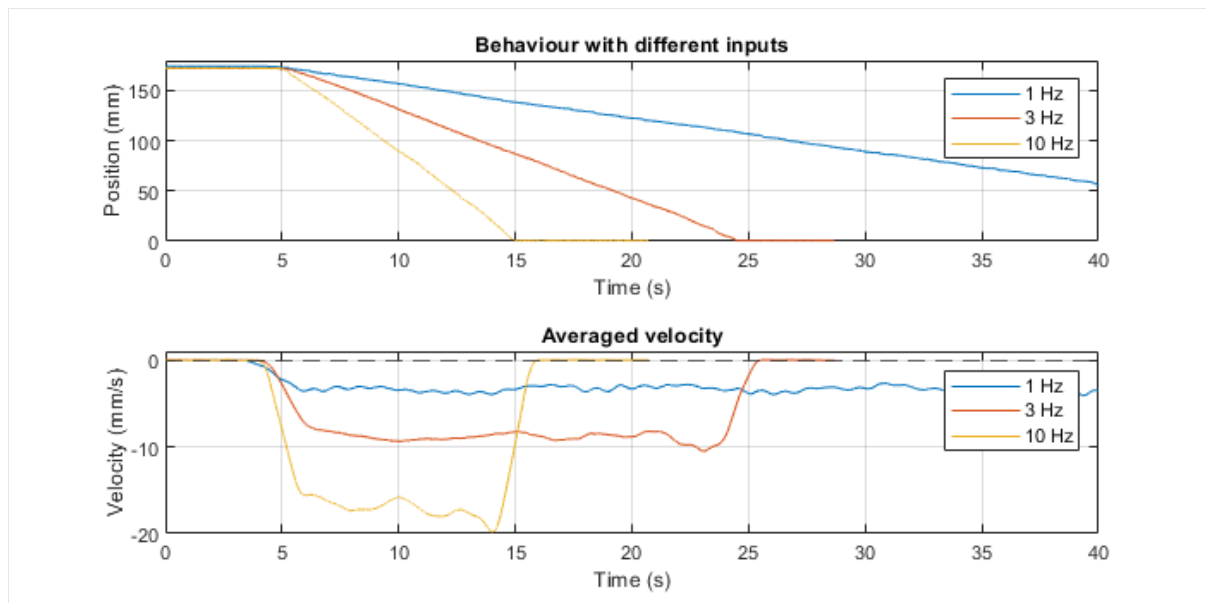


Figure 41 Test with different pulse rates

Tests show that the valve assembly can produce different flowrates and control the direction of an actuator. Correct size orifices should be added to individual vales to tune the behavior for a specific actuator.

### 3.1.4. Screw Propulsion Units

Screw propulsion units that are designed to be used on the Robominer consist of a water hydraulic motor, reduction gear, mounting parts, couplings, and the outer shell with thread. The rear mount



works as the torque holding member and acts as fluids paths for the water hydraulic motor. Due to the motor not having mounting points in the rear, an additional fixture is needed to mount the power unit. The mentioned components can be seen in Figure 42 and Figure 43.

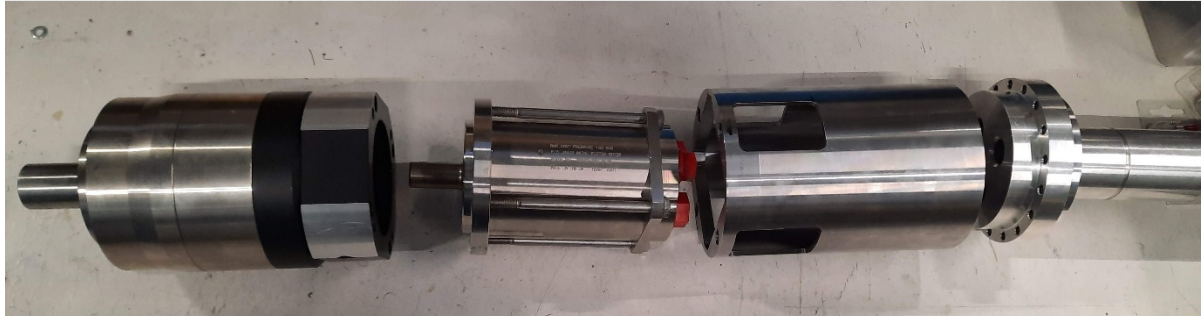


Figure 42 Screw internal components on workbench

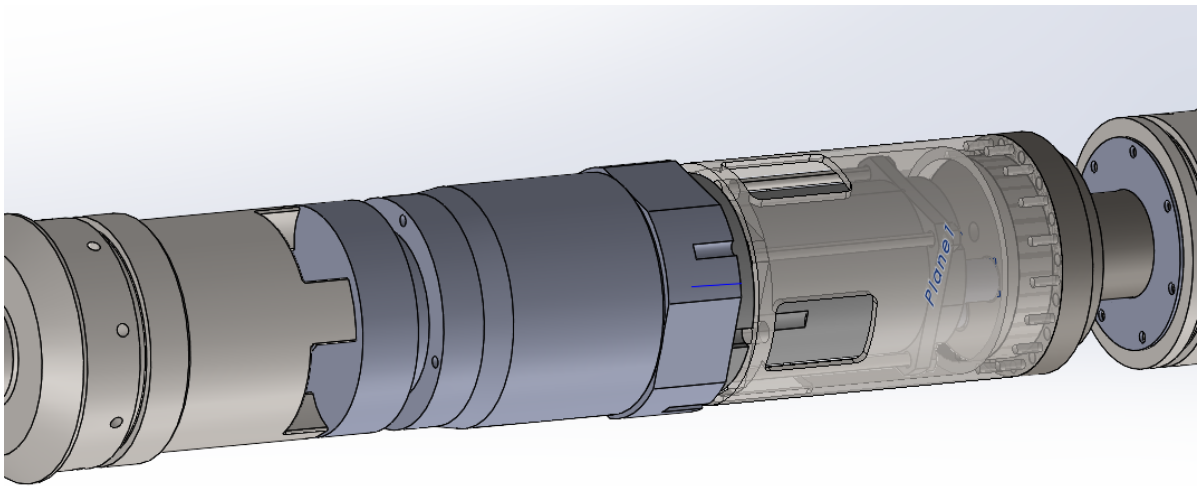


Figure 43 Screw internal components in CAD-model

The CAD model of the screw illustrates the parts in their final locations inside the screw: from right there is bearing housing to mount the outer shell with the thread, then there is fixed mounting shaft that also acts as hydraulic fluidpath for the motor, which is inside the semi-visible mount for motor. Next, marked with grayish blue color is the reduction gear with coupling which then transmits the drive to the outer shell of the screw. Total of 6 of these assemblies will be mounted on the RM1, four in the first module and two in the second module, as can be seen in Figure 43.

Test vehicle (Figure 44), dubbed as “the sled”, consists of two counter-rotating screw units attached to a frame and a pallet that is used to add load to the sled. The sled is attached to a wall with a wire cable that has a load cell to measure pulling force. The fixed location when cable is tight means that measured values are to be considered as “Bollard pull”, meaning the vehicle is not moving but the screws are slipping on the surface.

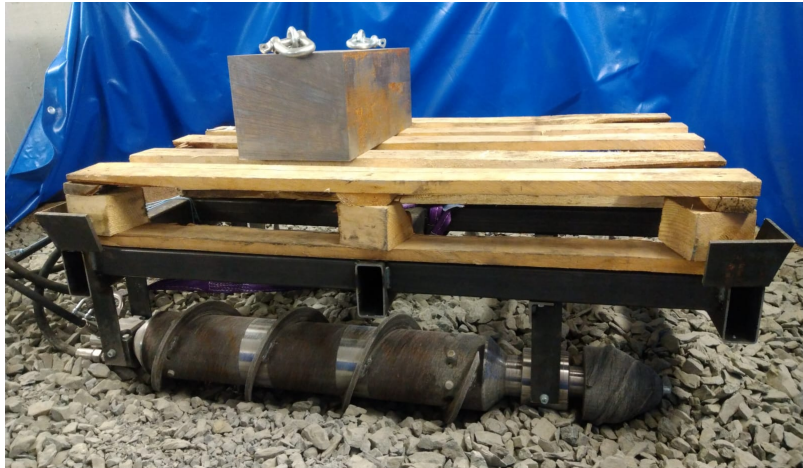


Figure 44 Screw sled with 200 kg load

Tests are run on loose gravel without the smaller particles in it, grain size being 16-32mm. The test sled was first tested without load (Figure 45), then additional load was added by setting a pallet and a substantial piece of steel, total weight of approximately 200kg (Figure 46 and Figure 47).

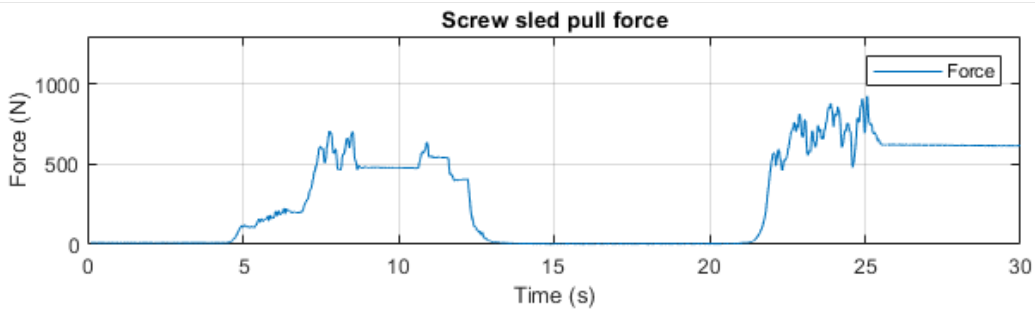


Figure 45 Pull test with bare sled

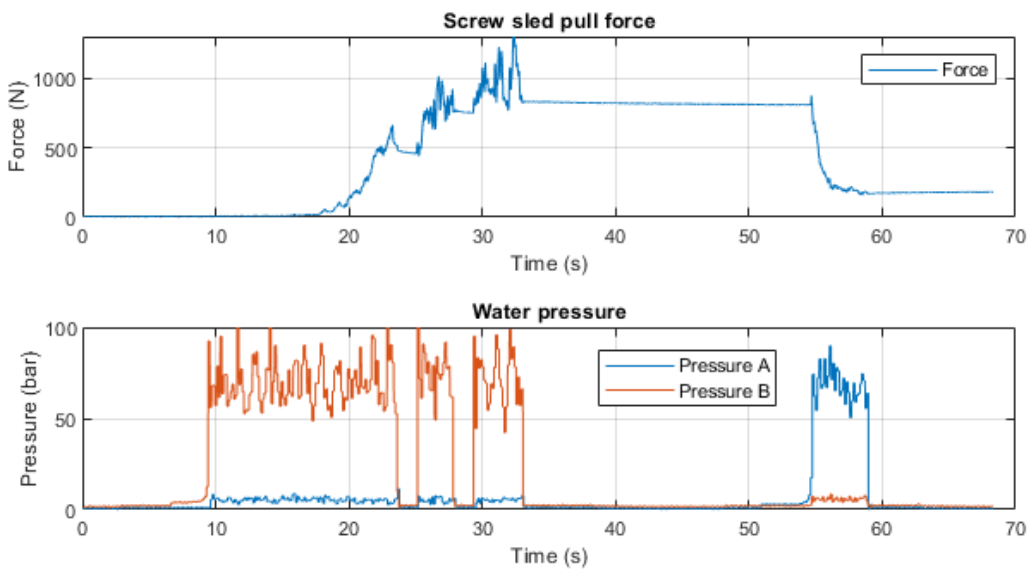


Figure 46 Screw sled with 200kg load, pull test with pressure logging

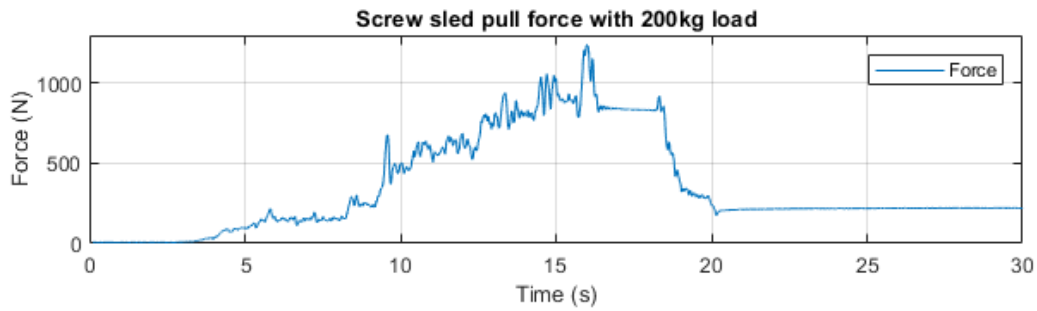


Figure 47 Pull test with 200kg of load on the sled

The results show a reasonable amount of pulling force, considering the looseness of the gravel used and the relatively small diameter of the propulsion screws. What can be seen in the data is related to the sinking or digging into the gravel; without extra load the maximum achievable force is reached almost instantly, and then the unit just spins in its place. With the extra load on top of the sled the initial force is lower, due to the screws sinking a bit into the gravel already before the slack was taken out of the cable. But with the extra load the screws sink more into the gravel, exposing more surface area for the thread to be in contact with the gravel and thus increasing the maximum pulling force to a higher number than without the extra load. The likely conditions in actual mine environment are harder material and have more solid edges of rock for the threads to grab, which should improve the unit's capability to provide traction force for the robot. Such test in more mine-like conditions with cut rock surface should be carried out to measure the performance in actual conditions, while also introducing more load than used in these tests.

The Figure 48 and Figure 49 illustrates both the pulling force and the pressure required for the motors to turn. Initially there is a section where the sled is moving and there is some slack in the cable for force measurement sensor, then the cable tightens, and the sled is stopped, and force increases. What can also be seen in this dataset is that the longitudinal force affecting the sled does not affect the force needed to turn the screws.

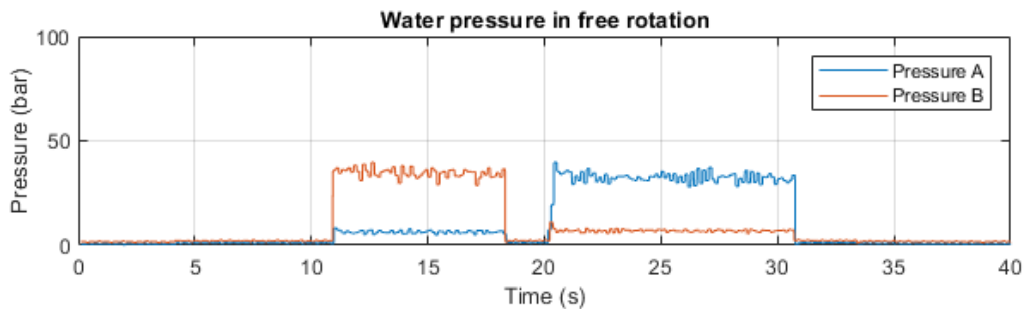


Figure 48 Screw motor pressures when rotating freely in air

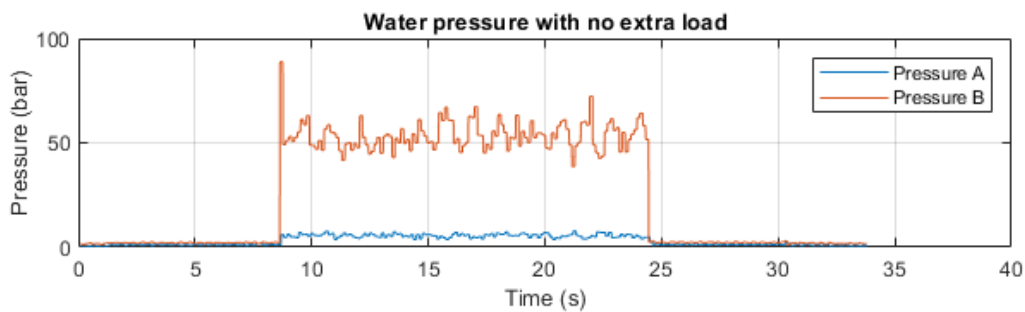


Figure 49 Screw motor pressures when running with no extra load

The pressure measurements show a positive result considering the motion capability of the robot; despite the motors being now connected in series, meaning the pressure for each motor is half of the measured pressure in graph, there should be no problem having enough force for the screws to rotate under full load of the robot. This can be estimated by observing the pressures needed in different load situations and noting that even with the 200kg load on the sled and screws entirely sunken into the gravel the pressure per motor is below 40 bar, meaning only less than one third of the available force is used (maximum pressure is 150 bar). Besides that, quite precisely half of that is needed for the screw to turn freely in air. The water hydraulic motor needs about 15 bar of pressure to start running, and the reduction gear and screw dust seals cause friction thus increasing the pressure needed for the screw to turn.

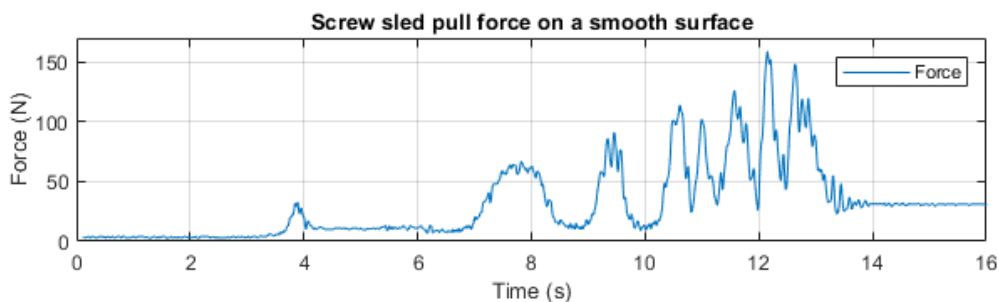


Figure 50 Pull force on a plywood surface

To compare the propulsion force, the sled was also tested on a plywood sheet and forces measured (Figure 50). The result show approximately a tenth of the pulling force seen on gravel, which is due to the threads not being able to generate traction in even surface with a low friction coefficient and propulsive force due to the screw moving the gravel is not generated either. It was also noticeable, that the sled was easy to slide on the plywood by hand, despite the sled weighing approximately 100kg without load. During the testing on the plywood, it was also noticed that on completely flat, smooth surface the sled moves sideways very much, and the behavior seems unpredictable.

To summarize the pull test results, the performance of the screw propulsion units on very loose gravel is not ideal, which was predictable, but they give reasonable amount of force on various loads and different surfaces. What still needs attention is to minimize the surface area of all the components that contact the gravel when the screw sinks, because these components cause significant drag when being dragged through the gravel. The controllability and traction on even low friction surface is challenging, but such surfaces in mine environment are so uncommon that it cannot be seen as a problem. The test on flat surface confirmed the assumption that the force produced is highly depending on the mechanical grip on the thread edge and the propulsive effect of the screw, and when that edge has nothing to grab or there is no medium to get propulsion, the force produced is low.

### 3.1.5. Hydraulic muscles

In D3.2 hydraulic artificial muscles (HAM) were envisioned to be used as linear actuators due to favorable characteristics. Unlike conventional hydraulic cylinders HAMa are actuators that consist solely of static parts, which improves their performance and reliability in harsh environmental conditions. Expansion of the HAM elastomer body under pressure cause the actuator to shorten, hence exerting a pulling force. When compared to hydraulic cylinders, HAM also present a higher power-to-weight ratio, but lower strokes can be achieved. In addition, it must be noted that only a pulling force can be achieved with a HAM, whereas a conventional hydraulic cylinder can operate in both pulling and pushing direction. Control of the actuators was envisioned to be through fast digital hydraulic valves using either digital hydraulic control principle or PWM/PFM control principle.

HAMs were tested in test rig shown in Figure 51. The test rig enables static and dynamic testing of the muscle by providing an artificial load generated by the oil hydraulic system and measurements needed to monitor the system. The main purpose of testing was to study HAM performance and to identify a mathematical model for it. Mathematical model would have been needed in control algorithm development.

Only low pressure HAMs (upto 15 bar) were tested due to unavailability of high pressure muscles. High pressure HAMs have been studied during recent years in rubber and actuator industry, but inspite of promising news they have not yet became commercially available.

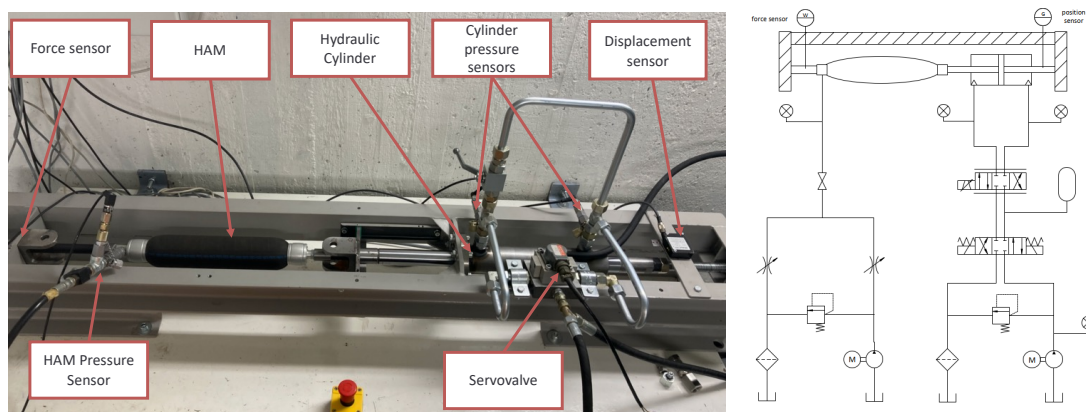


Figure 51 Hydraulic muscle test rig and its hydraulic diagram

HAMs exhibit, not only a highly non-linear behavior, but also a time-dependence (hysteresis phenomenon), mainly due to the internal friction of the braided rubber material. Both characteristics vary a lot in between HAMs of different brand and type. Therefore, there is no universal mathematical model for HAM and model parameters need always to be find by testing. Depending on the HAM (i.e. its structure) the force model needs to be chosen carefully. The force model is used in the controller to model accurately the pressure-force-displacement relationships.

Hysteresis can be clearly seen in Figure 52 where the force has been measured as a function of displacement (stroke) at actuation times varying from idle to 40 min. Also, some time dependence can be seen from curves having all different paths.

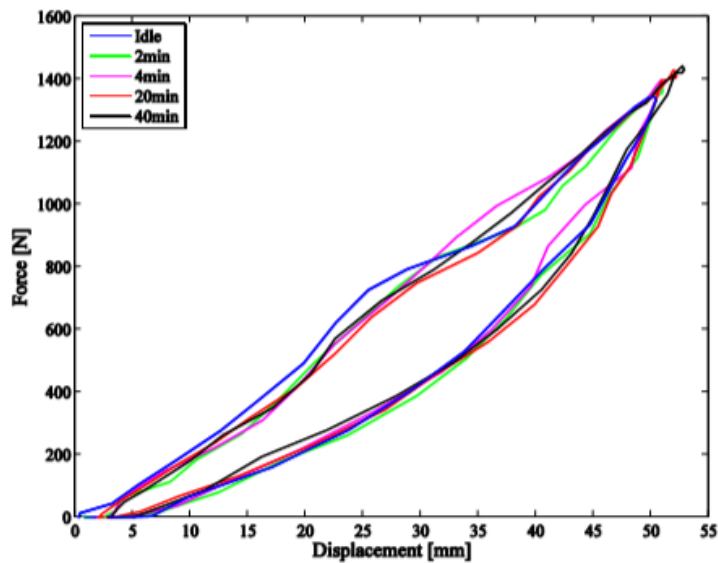


Figure 52 Hysteresis and time dependence in force vs displacement curve of a HAM

HAMs were tested to identify suitability of various models presented in the literature. The most suitable model with only small modifications as found to be so-called Andrikopoulos -model (Andrikopoulos G, Nikolakopoulos G, Manesis S (2015) Design and development of an exoskeletal wrist prototype in pneumatic artificial muscles. *Meccanica* 50). Figure 53 presents the measured forces and simulated forces. It can be seen from curves that the model fit is good.

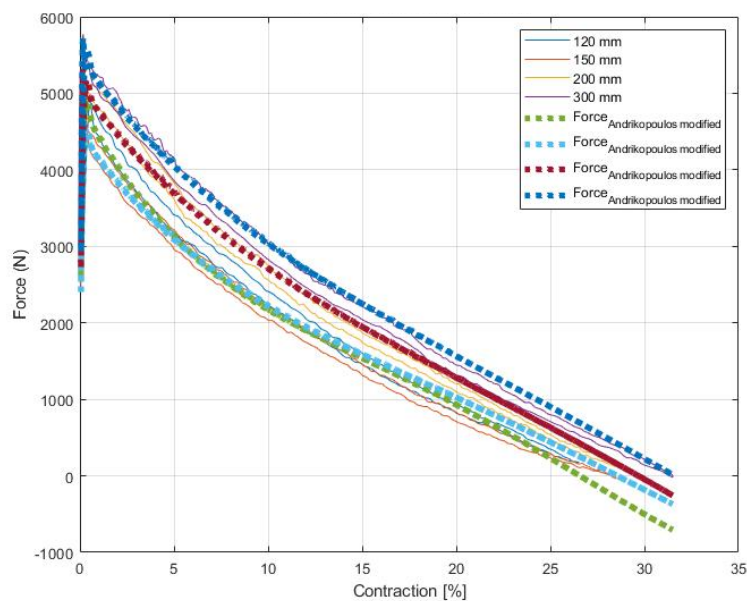


Figure 53 Measured force and modelled force at 6 bar operating pressure

During the testing it became evident that HAMs available as COTS components cannot provide high enough force to counteract forces generated by production tool operation. Higher capacity muscles have not yet entered to commercial market even though it was anticipated that they would be available by the time they are needed in Robominer.



## 3.2. Electronic Systems

### 3.2.1. Pressure Tolerance of Electronic Components

Pressure tolerance of electronic components is generally unknown parameter. Therefore, pressure tolerance of wide range of components were tested under hydrostatic pressure as a part of complicated circuit. Additionally, some components were tested individually. Multiple setups were constructed for tests.

To full scale circuits (assemblies and complete circuit boards), a pressure chamber was developed and constructed (Figure 54). The usable volume is 7 liter and maximum allowed pressure 700 bars. A cylinder bore was chosen so that a single-height (3U) Eurocard sized circuit board can be easily tested. (Kalle Hakonen, Testing electronic components and systems under hydrostatic pressure, 2021)

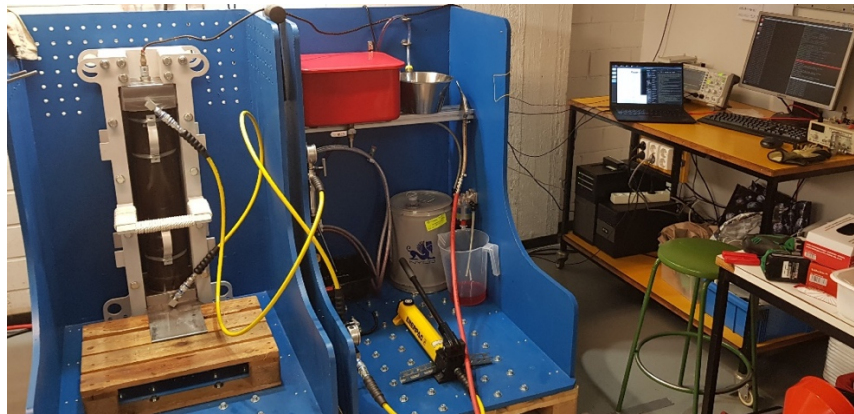


Figure 54 700 bar pressure chamber

To test the reliability of subassemblies a pressure cycling test system was developed and constructed (Figure 55). Pressure cycles are used to generate the fatigue and general ageing encountered in prolonged use during the test. With this setup, the specimen being tested is pressurized and depressurized in two-second cycles.

Lithium polymer batteries were tested under the hydrostatic pressure of 500 bar (Figure 56). Five different cells from three different manufacturers were tested. Given capacity varied from 190 mAh to 1000 mAh. All the tested cells were usable under the aforementioned pressure. The usable capacity of the cells decreased mainly by less than 30 %. These measurements proved that LiPo-cells can be used in RM1. (Anton Wallendahl, Litiumpolymeeriakkukennojen ominaisuudet hydrostatisessa paineessa, 2021)



Figure 55 Pressure cycling test system



Figure 56 Lithium battery cell after pressurized in oil

Four different types of temperature sensors were tested under the hydrostatic pressure ranging from 1 bar to 600 bar. All the tested cells were usable under the aforementioned pressure but there is a pressure dependence in them. Pressure dependence is presented in Figure 57 (Tomi Haapanen, Effects of high pressure on temperature sensors, 2021)



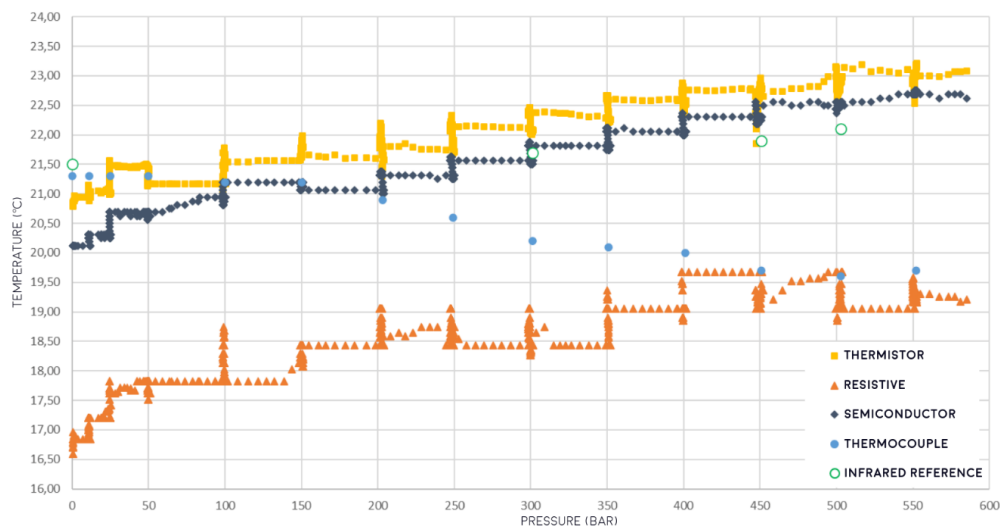


Figure 57 Pressure dependence of different temperature sensors

The use of fiber optic temperature sensors was investigated. While specific pressure dependence was not found, fiber optic sensors react to the pressure in addition to temperature. Although the sensor is robust and mechanically simple, the equipment needed to interpretation of results is complicated and possibly too hard to protect in the ROBOMINERS context. (Eetu Tiiri, Kuituoptiset lämpötila-anturit – paineriippuvuus ja käyttökohteet, 2022)

Single-board computer was tested as a whole system. Operation of SBC under pressure was studied by monitoring the communication between two SBCs, the interpretation being when communication between computers was successful, they work. Studied SBCs were submerged in pressurize dielectric oil. The dielectric oil is frequently used with underwater electrical equipment. The compressibility of the oil is low compared to gases, and it also minimizes reactions between pressurized gases and equipment. Tests were executed, and even unprotected SBC was able to tolerate the pressure of 20 MPa over 164 h without failure. At higher pressures, the system was working limited time, and there is no proof, which was the single point of failure. Still, it was evaluated to be a crystal as the strengthening of the case allowed to push pressure higher for the whole system under inspection. According to earlier research, SBC chosen for tests did not include the most vulnerable capacitor types, and the quartz crystal was expected to limit the pressure. After measures were taken to protect crystals, short term pressure tolerance of the board was increased significantly. (Kalle Hakonen, Testing electronic components and systems under hydrostatic pressure, 2021)

SBCs tested were Olimex A64-OLinuXino open-source hardware boards. Open-source hardware allows study of used components and thus testing them leads to list of components proven to pressure tolerant. Even though RM1 prototype will not be used deep underwater, circuits are designed, and components are chosen so that it is possible to use boards directly under pressure. Table 3 shows components in SBCs with a prove pressure tolerance. Using this test data and testing individual components separately allowed constructing pressure tolerant circuit boards for RM1. (Kalle Hakonen, Testing electronic components and systems under hydrostatic pressure, 2021)

All circuit boards designed for the robominer, were designed with the knowledge about pressure tolerance gained previously. Although only pressure sensor was tested in the pressure chamber after constructions.

Table 3 List of component types and packages pressurized to 50 MPa as a part of a functioning single-board computer.

Component type	Package	Component type	Package
Capacitor (ceramic)	0402	Crystal	MC306-HS
	0603		HCX-4S
	0805	Diode	0603
	1206		SOD-123
Resistor (thick film)	0402	FET	DO-214AC
	0603		DO-214AA
	1206	SOT23	
	4X0402	IC	DFN2x2-6L
	4X0603		SOT23-5
Inductor (ferrite core)	0805		SOT23-6
			SOT223
Inductor (ferrite core, open)	CD32	Fuse, PTC	QFN48
	CD43		QFN68
	7 × 8 mm		FBGA96
			FBGA396
			1206

### 3.2.2. Valve controller board

All actuators in the RM1 are water hydraulic. The actuator control utilizes so-called digital hydraulic principle, i.e. the flow is controlled with simple 2/2-valves driven by electromagnetic coils, and solenoids. The control of the coils is distributed to multiple identical circuit boards (Figure 58). Boards are independent units which contain a SBC for computing and communications and thus they are in the point of view of the robotic control individual ROS-nodes. One board can control 16 solenoids and it can read simultaneously 8 analog pressure inputs. In addition, 4 position sensors can be read via SENT-bus. Ethernet is used for communication with the system.

Valve controller boards are based on individually tested components and they were used in all laboratory testing involving valve controls thus separate testing of them is not required.

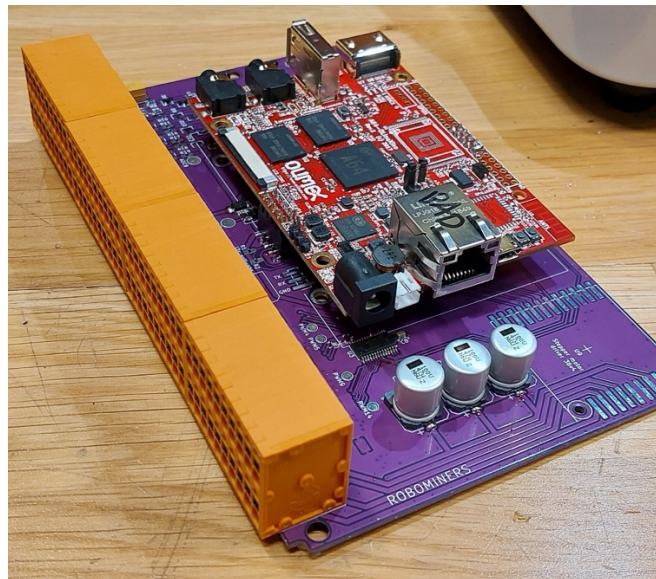


Figure 58 Valve controller board

### 3.2.3. Electronic pressure regulator

The powerpack will provide 150 bar pressure to the robot, but there are some actuators that require lower pressure of approximately 40 bars. Ideal solution would be to use a traditional hydro-mechanical pressure reducing valve to limit pressure, but availability water hydraulic pressure reducing valves capable of lowering pressure from 150 to 40 is limited, their dynamics are generally bad and size is too big. Thus an electronic pressure regulating valve (Figure 59) was developed to maintain the desired pressure level.

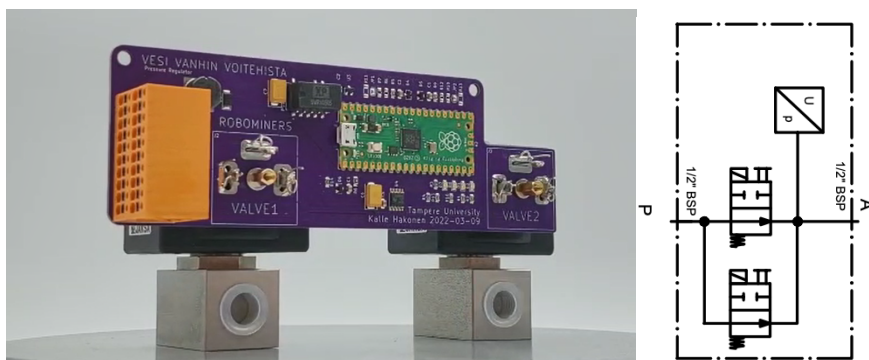


Figure 59 Pressure regulator circuit board and hydraulic diagram

The regulator works by measuring downstream pressure and attempting to maintain a target pressure with two solenoid valves. Valve opening algorithm and valve restrictions can be tuned to accommodate for required flowrate. Valve switching does create vibration that is reduced by equipping the system with accumulators.

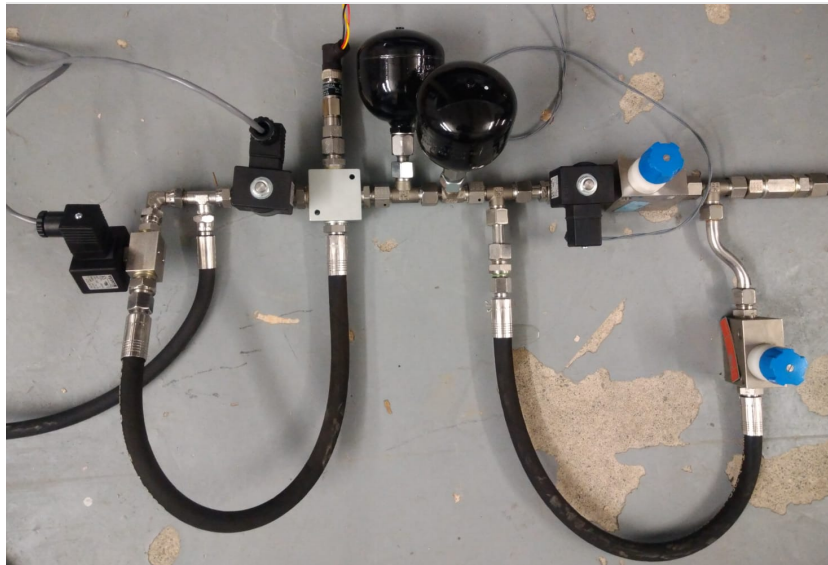


Figure 60 Pressure regulator test setup

The test setup (Figure 60) used to test the regulator is constructed of two inlet valves that the regulator controls, pressure sensor, accumulators, an outlet valve, and a biasing valve to test different flowrates. The outlet valve is a solenoid valve with a throttle valve in series that can be actuated to test how the regulator responds to a change in flowrate. The biasing valve is a throttle that is used to add a flowrate bias.

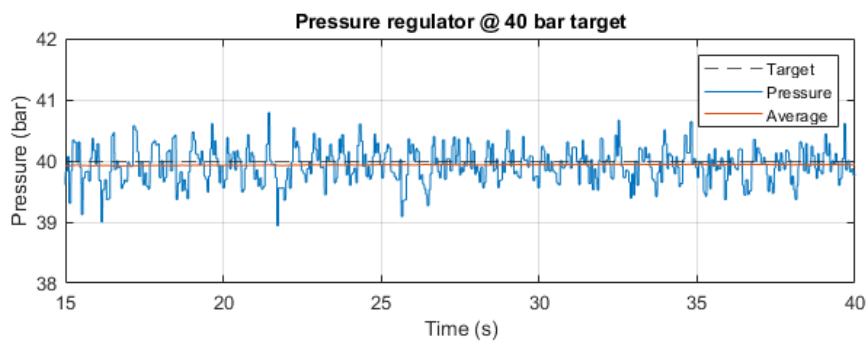


Figure 61 Pressure regulator with static flowrate

The regulator was first tested with a static flowrate by keeping the outlet valve fully open and biasing valve closed (Figure 61). This results in approximately 4 liters per minute flowrate through the outlet. Figure 61 shows how the regulator behaves at 40 bar target pressure. The accuracy is 1 bar, meaning that at 40 bars the overshoot is only 2.5 %. The average pressure stays close to the target and has virtually no error.

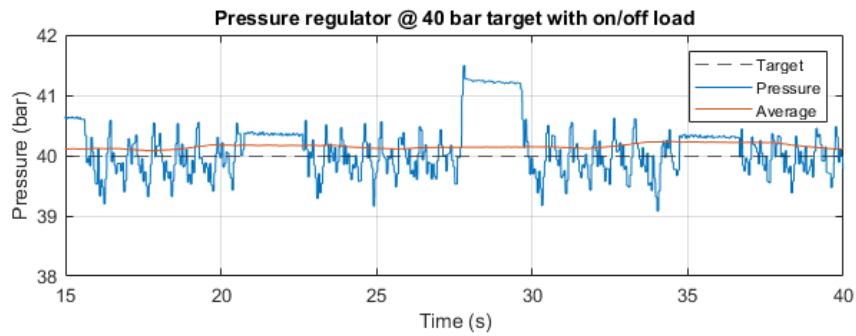


Figure 62 Pressure regulator with on/off load

Next test was to see how the regulator responds to a changing flowrate. This was done by switching the outlet valve periodically. As can be seen from Figure 62, while the valve is open the behaviour is the same as in Figure 61 as the conditions are identical. When the valve is closed, pressure increases slightly above the target value. On some occasions the increase is bigger as seen at around 28 seconds in Figure 62. This is caused by response time of the regulator and the inlet valves. If the inlet opens just as the outlet closes, it takes enough time for the valve to close for the pressure to increase slightly. The highest overshoot encountered was around 1.5 bars which is low compared to commercial hydro-mechanical valves. Furthermore, the regulator will be used in conjunction with a pressure relief safety valve that can take care of dangerous pressure spikes.

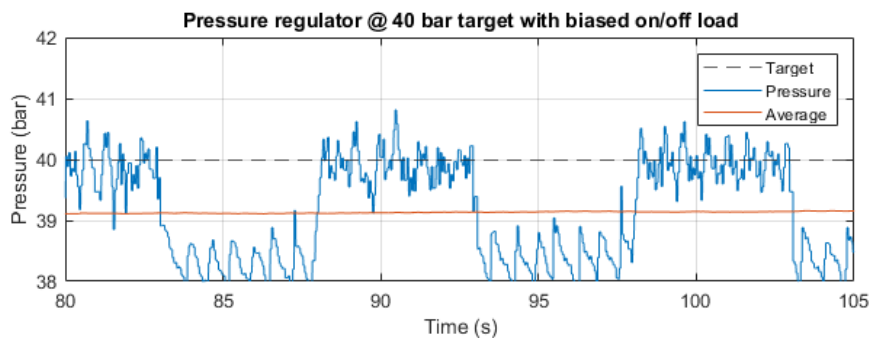


Figure 63 Pressure regulator with biased on/off load

In Figure 63 the biasing valve is opened to let out around 4 liters of water per minute and the outlet valve was opened periodically. So, flowrate with outlet valve closed is 4 liters and 8 liters when open. And again, the 4 liters per minute flow gives similar pressure behavior as the static test in Figure 61. Now when the outlet is opened and 8 liters per minute is let through, pressure drops to between 39 and 38 bars. This is a 5 % error and while not a problem begins to show the limitations of the rudimentary control algorithm used in the regulator.

These results are promising and show that the electronic pressure regulator does work and is able to maintain a safe pressure for the actuators which require lower pressures. Further tuning could be done to reduce error on higher flowrates. Theoretically the regulator is able to produce a maximum flowrate of around 16 liters per minute, set by the flow coefficients of the inlet valves and supply pressure. It is enough to serve flowrate needs of low-pressure actuators in a single Robominer module.

### 3.2.4. Pressure Tolerant Sensors



The control of RM1 is highly dependent on pressure sensing in its actuators. Approximately 40 pressure sensors will be installed on it. A novel way to measure pressure with a sensor with no moving parts and based on COTS electronic components was developed and tested (Figure 64). The novel sensor is small and its component count is minimized for reliability and price. The sensor measures absolute pressure.

Sensors were tested in the pressure cyler, varying the pressure from 5 bars up to 160 bars. In total, 2500 cycles were executed. The reference sensor was Kulite ETM-375M-350BAR. Figure 65 shows the comparison between the pressure sensor and the reference sensor output. It can be clearly seen that dynamics of the novel sensor are somewhat slower, but yet satisfactory, and the accuracy is good. Sensors developed for ROBOMINERS performed as expected. According to the test, the current sensor design can be used in the RM1.

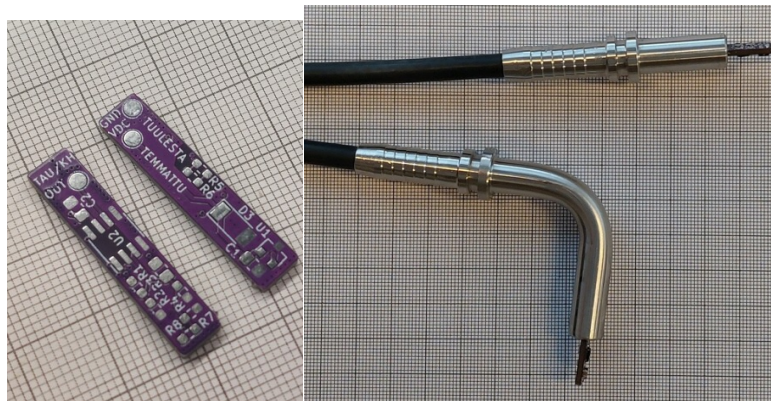


Figure 64 Pressure sensor circuit boards and completed sensors

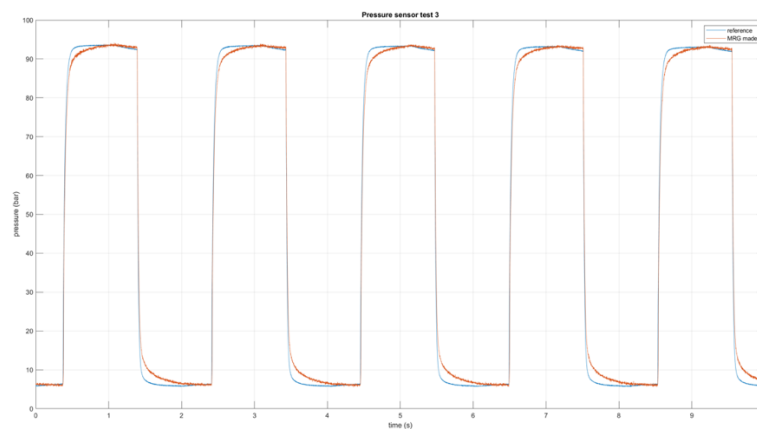


Figure 65 Reference sensor and new experimental sensor comparison.

It is also important to know angles of several joints and lengths of hydraulic cylinders on the robot. As a high number of sensors is used in a rough condition, the sensors should be simple and robust. The sensors also have to be able to communicate through couple of meters of cable as the sensors are located somewhat far from the controllers, this rules out most simple and common ic2 sensors and analog sensors.

Position sensor selected is Melexis MLX90366, that can measure absolute rotary and linear position based on magnetic fields. The sensor communicates using SENT (Single Edge Nibble Transmission) protocol requiring only 3 wires and works for lengths up to 5 meters according to SAE J2716-2010. All

other electric components but the sensor itself are placed inside the robot. Thus, only the sensor is exposed to the elements. The same sensor is used for rotational and linear movement.



Figure 66 Magnet mounted on a servo motor and the sensor

The sensor accuracy was tested by rotating a diametrically magnetized disk magnet mounted on a servo motor with a rotary encoder (Figure 66). The stated linearity error for the sensor is  $\pm 1$  degree and the tests confirmed this. A simple test program was created to compare sensor reading to servo position and the highest deviation was slightly over one degree. The sensor can be mounted in almost any orientation even with an offset to the magnet and is able to get a good reading even 2 cm away. The magnet however needs to be diametrically magnetized and rotating on its centre axis as the sensor is sensitive to magnet misalignment.



Figure 67 Protective sensor enclosure

The sensor will be exposed to the elements, so it needs a protective enclosure. As the sensor is based on magnetic fields, the enclosure needs to be made from materials that don't interfere with that. A test enclosure was made by casting the sensor in epoxy inside an aluminium tube. The enclosure also gives the sensor required pressure tolerance (Figure 67). Based on tests, no perceivable difference was found compared to a bare sensor IC.

### 3.2.5. Communication Network

Modules inside the ROBOMINERS mining robot interact via Ethernet. The same communication bus is extended from the robot module of the RM1 up to the ground control station. Connections to possible data centers are handled by the GCS.

The network media between GCS, underground stations, and the robot itself is a single-mode optical fiber. It is immune to electrical interference and provides sufficient bandwidth over the distance. Achievable distance is dependent on the optical fiber, connectors, and optical endpoint capabilities. In

RM1, endpoints are network media converters, converting the electrical network to optical and vice versa.

Converters used specify:

- Transmitter Power -9 - -3 dBm
- Receiver Sensitivity < -22 dBm

giving worst case link budget 13dBm.

Optical fiber and connectors are COTS military field cables. Attenuation of the fiber is defined here to 0.35 dBm / km of fiber, 0.1 dBm / splice in the fiber and 0.75dBm / connector. As the cable is supplied on the reels of 300 m this leads to following losses:

- 300 m (one reel): 4.8dBm
- 600 m (two reels): 5.1dBm
- 900 m (three reels): 6.9dBm
- 1200 m (four reels): 8.7dBm
- 1500 m (five reels): 10.5dBm

Thus, when compared to the worst case link budget, 900m distance between GCS and the underground station leaves a safety margin of 6dBm which is estimated to be sufficient.

To test communications network two parallel, but connected, networks are constructed (Figure 68). One is primarily for the RM1 operation and control. The second one is for the infrastructure, video surveillance, and human interactions during development. Having a separate network for control and support functions allows higher security levels and more bandwidth for the physical action of the robot. Laboratory tests proved the reliability and operation of the network with minimal communication losses.

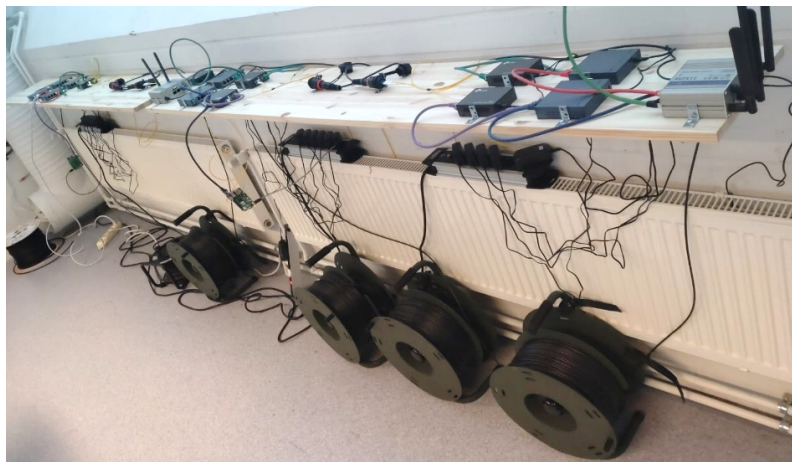


Figure 68 Communication network test setup



## 4. EFFECTOR AND MULTICOUPLING LABORATORY TESTS

The effector consists of the boom and the production tool (Figure 69). Boom is used to manipulate the production tool and it is actuated by four water hydraulic servo actuators. Multi-coupling (**Error! Reference source not found.**) provides in RM1 only articulated steering functions. It is controlled by three water hydraulic servo actuators. All actuators are similar. This document presents the laboratory testing of servo actuators only. The boom and multi-coupling assemblies in whole will be tested in complete RM1 tests.

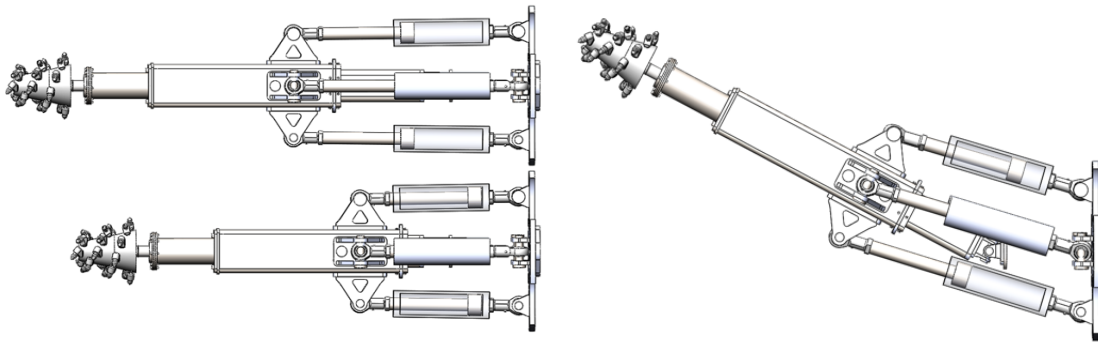


Figure 69 Boom assembly

### 4.1. Boom and Multi-coupling Actuation

The boom and multi-coupling are actuated with water hydraulic cylinders controlled with the 4-way valve assembly introduced in 3.1.3.

Cylinder positioning accuracy was tested with small 50 mm steps (Figure 70). Test was run with a simple proportional control with different gains depending on direction to account for the differences in effective cylinder piston area. With this setup the position reached the target value within 5 seconds with accuracy of 2 mm. The error is constant in the direction of the load. This could be improved by changing the control parameters based on load that could be calculated from cylinder pressures. Gains can also be adjusted to match the speeds better.

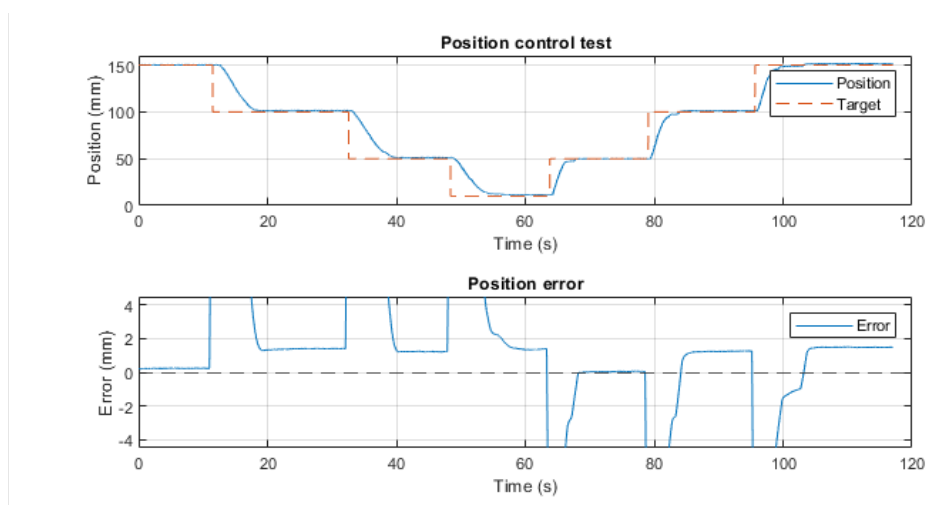


Figure 70 Positioning accuracy test with small steps

Proportional control gain used in the tests was low and the cylinder does not reach its maximum velocity. It is presumed that the drilling operation does not require fast movements, so these faster speeds from the cylinder are unnecessary. This means that the valve assembly can be adjusted by lowering maximum flow rate, improving control resolution (smaller movement per pulse) at lower cylinder speeds. This would result in more accurate position control.

During drilling the position of the production tool must be able to follow a path. This was tested by giving a changing target for the position control loop. Ideally a more sophisticated control could be used for following a trajectory, but proportional control loop is simplest possible and thus allows testing the properties of hydraulics instead of controller. Also, although not ideal, proportional control can still give good enough results when the actuator is moved at slow speeds.

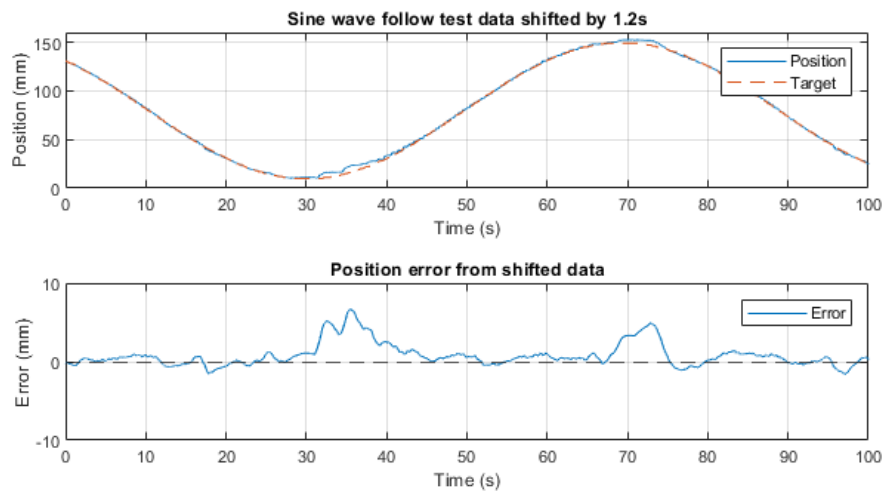


Figure 71 Path follow test data shifted by 1.2 seconds

Figure 71 shows how the position follows the target's shape. Position error stays well near zero and deviates only when changing direction. The error on direction change is caused by imbalance in accumulator charge levels induced by the load force. This can be compensated by introducing pressure feedback loop into the final construction of the boom and multi-coupling control. Overall the results are satisfactory and show that even with the simplest possible control loop the control accuracy and speed are good for both boom and multi-coupling operation.

## APPENDIX 1 REQUIREMENT SPECIFICATION WITH CHANGELOG

Tables below present the requirement specification originally published in D3.2 with 'changes' column added. Changes column (in red) shows the changes to original specification and their effect on the functions or capacity of RM1.

### Locomotion

Articulated screw propulsion with four screw units	High traction	All screws are pushed against tunnel walls	
	Reliability and survivability	Better compared to fully articulated legs, track or wheels	
	Modular		

### Production capability

Extraction capability	0,2 m <sup>3</sup> /h solid rock	
Rock transport capacity	0,2 m <sup>3</sup> /h	
Excavation capacity	Max. 100 MPa uniaxial compressive strength	

### Operational Case Scenarios

Three case scenarios	Operating abandoned mines with known remaining unfeasible resources	Example for scenario: Neves-Corve	
	Ultra-depth	Example for the scenario: Kupferschiefer, Fore-Sudetic Monocline	
	Small deposits uneconomic for traditional mining	Example for the scenario: United Dows project, Cornwall	

### Ambient Conditions

Descent	45 ° to vertical downwards following the ore base	Design: yes. To be verified in lab tests
Ascent	45 ° to vertical upwards following the ore base	Design: yes. To be verified in lab tests
Maximum operating depth	Full scale proto 50 m (5 bar) (Demonstration up to 40 m)	

	Design solution up 5000 m (500 bar)	With current technology up to 1000 m (100 bar). With minor modifications up to 5000 m (500 bar).
Temperature	Full scale proto from 0°C up to 45°C	
	Design solutions from 0°C up to 85°C, with cooling water circulation 125°C	

**Production method**

Production tool	Drilling and blasting/ hydrocracking		
	Grinding		
	Interchangeable		
Size	Dimensions		
	Shape		
	Weight		
Crusher	Max particle size		Not implemented. Reason: Not needed in RM1.
	Capacity	0,2 m <sup>3</sup> /h	
	Power	7,5 kW	

**Manipulator Arm for Production tool**

Size	Dimensions	TDB (Depends on production tool)	1,3 m + 0,25 m stroke + 0,36 m joint extension
	Weight	TDB (Depends on production tool)	170 kg (includes cylinders, casing, tool, gear, motor, reducer coupler, bearings)
	Reach	Robot radius + 0,5 m	Robot radius + 0,31 m
	Effector weight	TDB (Depends on production tool)	20 kg (just tool)
Function	DOF	2 - 3	3
	Joints	1 - 2	1
	Actuators	2- 3	4
	Sensor	Sensor for the mineral vein	2 sensors for the mineral vein, 4 angle sensor for position

**Maneuverability**

Turning radius	In open area	In its place	
	In a tunnel	0,5 m + diameter of the robot	Theoretical minimum 2,3 m. To be verified in tests
Climbing capability	Max ascent and descent	90-degree vertically	Design: yes. To be verified in tests
	Stepping capability	Can step over obstacle which is 45% of the robot's height	Design: yes. To be verified in tests
Degrees of freedom	One module	4 DOF	
Movement speed	Transport	0,25 m/s = 0,9 km/h	
	Mining	TBD (Depends on production tool)	
Environmental adaption	Tunnel	Mostly working the hole made by itself	
	Open pit	Transport	
		Starting new tunnel	
	Fully/partially submerged	Mud/slurry	
		Water	
	Open Land	Transport	
		Starting new tunnel	

### Energy

Electric power	Constant electric power through tether	48 VDC/ 3A, peak power from the batteries	24 VDC/ 10A, peak power from the batteries. Reason to change: Simplify design due to components shortage.
Water hydraulic power	Through tether*	30 kW (85 l/min @ 160 bar)	30 kW (105 l/min @ 150 bar)

\*Prototype only

### Mechanical Design

Body ( one module)	Length	<1 meter	1,12 m
	Diameter	Ø0,8 m (cross-section area of the tunnel 0,5 m <sup>2</sup> )	Ø0,8 m
	Target weight	1500 kg	

Movement system	Screw propulsion		
	Legs	Actuators - Hydraulic artificial muscles	Actuators - Hydraulic cylinders. Reason: COTS high pressure muscles not available yet
		Capability to step over an obstacle	
		Capability to increase traction	
Module coupling	Max 6 DOF active coupling		3 DOF. Reason: 6 DOF not needed in RM1 and similarity
	Capable to articulated steering between modules		
	Module docking function	Relative locating of modules	Not implemented. Reason: Not needed in RM1.
		Power coupling of modules	Not implemented. Reason: Not needed in RM1.
		Close range wireless comms	Not implemented. Reason: Not needed in RM1.
Anchoring	Anchoring capability to increase traction	10 000 - 15 000 N total traction force	Design: yes. To be verified in tests
Underground support module	Electric power	48 VDC via 4 - 6 mm <sup>2</sup> cable	24 VDC/ 10A, see chapter 2.3.3
	Hydraulic power	87 l/min @ 160 bar via - 16 (DN25) hose	87 l/min @ 150 bar, no effect on the performance
	Extracted rock transport	Crushed rock 0,2 m <sup>3</sup> /h + water over 0,2 m <sup>3</sup> /h	

**Reliability and Availability**

Durability	System robustness	One year in mine conditions*	
	System endurance	Robot has to be able to self-replace wear parts*	

		Robot has to carry wear parts *	
		One-year autonomous operation time *	
Survivability	Robot must be able to self-recover	Rock collapse etc.	Not implemented. Reason: Not needed in RM1.
	Minimum is that robot should be able to transmit its location and status		Not implemented. Reason: Not needed in RM1.
	Falling	Falling height 3 times its own diameter	Not implemented. Reason: Not needed in RM1.
	Temperature changes	Puncturing geothermal well or stream wall	Not implemented. Reason: Not needed in RM1.
	Flow velocity changes	Puncturing subterranean stream wall	Not implemented. Reason: Not needed in RM1.
Damage tolerance	No single failure of main components should render robot in operational		
Fail safe	Self-recovery from failure in main components	Communication fiber (military grade and double fiber)	
Condition monitoring	Self-aware of failures		

\*Final design solution, not prototype

### On board Electronics

Software	Orchestration	
	Tool usage	
	Power control	
	Communication	
	Coupling	
	Locomotion	
	Sensor interfacing	
	SLAM	

System electronics	Computers	
	Communication	
Sensor electronics	Sensors	
	Adapters (communication)	
Power & Control electronics	Power for systems	
	Battery Management	
	Control electronics (actuators)	
Communication electronics	Internal communication	
	Module communication	
	External communication	

**Hardware Interface**

Wired optical ethernet (external)		
Wired ethernet (internal) RJ45		
Wireless ethernet (external)		
Wired low power electricity, 5V 3A		
Wired high power electricity, 48V 3A		Wired high power electricity, 24V 10A. 100A max 1 min, 1:15 duty ratio.
Wireless low power electricity, 5V 1A Qi		
Hydraulics	Pure water without additives @160 bar	